

Question 71a: *Core 3-D Flow and Void Distribution (Page 4-85, EMF 2103). Comparison to the THTF and GE Level Swell data, for example, are high pressure tests and do not represent PWR reflood conditions. The GE data does not apply to rod bundle drag. On the other hand, specific FLECHT boil-off or reflood data are applicable to voids in bundles at low pressure (FLECHT-SEASET Test 35658, for example).*

Response 71a: In addition to the high pressure void distribution comparisons for the THTF and GE level swell tests, void distribution comparisons have been made for low pressure reflood tests. The void distribution comparisons for FLECHT-SEASET and FLECHT SKEWED reflood tests are represented by the calculated and measured differential pressures between 72 and 84 in. displayed in Figures 3.3.71 to 3.3.79 of EMF-2102(P) Revision 0. Note particularly that code-data agreement is excellent after the region between 72 and 84 in. is completely quenched. This demonstrates the wet-wall (pre-CHF) interphase friction model is applicable and adequate for both high pressures (THTF Tests) and low pressures. The void distribution above the quench front is dominated by the dry-wall (post-CHF) interphase friction model. The differential pressure plots show that (1) the calculated liquid fraction far above the quench front is lower than the measured and (2) the calculated liquid fraction near the quench front is higher than the data for injection rates below 1.5 in/sec and lower than the data for injection rates higher than 3.0 in/sec. This void distribution pattern is consistent with the clad temperature history at around the 78 in. elevation.

The key factor in determining the clad temperature (and PCT) is the void (or more properly, liquid) distribution. The key question to ask is, "Where is the water?" The lower liquid fraction (in comparison with the data) far above the quench front and the generally lower core inventory calculated (Figures 3.3.89 -3.3.97 of EMF-2102(P) Revision 0) indicates that insufficient liquid is retained at elevations far above the quench front and most of the liquid drops carried away from the quench front are carried out of the core. This tends to produce higher clad temperatures during the temperature rise period and hence, conservative (high) PCT as demonstrated by most of the assessments of the reflood separate-effects and integral effects tests reported in EMF-2102(P) Revision 0. The accumulation of more liquid in the region immediately above the quench front results in a quench time closer to the data (Figures 3.3.104 -3.3.109), in spite of higher PCT. The picture of void distribution for the post-CHF region is not perfect and is not as good as that for the pre-CHF region, but it is adequate and conservative for licensing applications.

Question 71b: *Regarding Core 3-D flow distribution, the SCTF comparisons, especially at the higher elevations, indicate underprediction of peak temperatures and quench times that are early by 200 – 300 seconds for transients with 500 second heat-up times. Additional justification is needed to demonstrate that the clad oxidation is bounded. While these are low temperature tests, the early quench time predictions will significantly affect oxidation and the uncertainty may effect the error methodology. Discussion is needed regarding how the 200 – 300 second early quench predictions are factored into the uncertainty in oxidation calculations. There should also be discussion of the lack of a model for film boiling as a function of distance from the quench front which would improve the quench time predictions. This discussion should also address the reasons for the discrepancies in quench time predictions and underprediction of PCTs. The S-RELAP5 code predicts large oscillations in the void fractions in the core (see Fig. 3.11.47 of EMF-2102, for example). Discussion is needed regarding the oscillations and their effect on super heat and clad temperature underprediction. The discussion should also address the*

consequences of the oscillations with respect to the reflood behavior the potential bias of these oscillations to lower PCT.

Response 71b: Framatome ANP has limited the use of the SCTF comparisons to demonstration of the adequacy of the code to calculate radial power distribution effects. The reason for this is that many assessments of S-RELAP5 against experimental data were made, and for essentially all assessments except the SCTF, the code results versus measured data exhibited a consistent conservative pattern for predicting heat transfer and PCT. For reasons not yet understood, the SCTF assessment yielded acceptable PCT comparisons but did not show the same prediction pattern for heat transfer. Framatome ANP believes the predictive capability of S-RELAP5 should be established based on the consistent predictive trends with other assessments and not the SCTF tests.

Question 71c: *Liquid Entrainment.* While the entrainment is overpredicted for the CCTF tests, overprediction coupled with drop size could bias the steam temperatures in the channel to low values if the drop size is too small. Please discuss how the S-RELAP5 model predicts the steam super heat for these tests (at selected elevations starting at locations near the quench front) and the reflood data presented in EMF-2102. How does the void fraction influence the steam super heat and dispersed flow film boiling heat transfer when the entrainment is over-predicted for the tests? Included in the discussion should be the topic that excess entrainment does not lead to propagating errors into the film boiling model and a non-conservative impact on PCT.

Response 71c: The tendency and consequence of the post-CHF interphase friction model to retain less liquid at elevations sufficiently far above the quench front are discussed in the Response to Question #71.a. Such a tendency is the most significant contributor to the calculated higher PCT in most assessment cases, regardless of whether excessive liquid entrainment is present in a calculation.

For the four CCTF tests, the good agreement between the calculated and measured core differential pressure (Figures 3.12.29, 3.12.56, 3.12.84 and 3.12.112 of EMF-2102(P) Revision 0) suggests that the overall void (or liquid) distribution is properly calculated and the liquid carry-out is not excessive. Because the steam temperature instrumentation did not correctly measure the superheated steam temperature in a steam-water mixture environment, as pointed out in Section 4.3.1.12 of EMF-2103(P) Revision 0 and Section 3.12 of EMF-2102 (P) Revision 0, it is not possible to assess the performance of the code calculation of steam temperature against the data.

Generally speaking, the two most important factors influencing the steam superheat are (1) the heat transfer to steam and (2) the vapor generation rate. A lower calculated steam temperature may be caused by lower heat transfer to steam or higher vapor generation rate or a combination of the two. The vapor generation rate depends on the interphase heat transfer model and the amount of liquid; therefore, excessive entrainment, even if calculated, does not necessarily imply higher vapor generation rate or lower steam temperature. Also, a lower steam temperature does not necessarily imply a higher heat transfer rate and a lower PCT. The two-fluid heat transfer model requires the partition of heat transfer to liquid and vapor, but currently there are no data or theory available for accurate modeling of the partition. Forslund and Rohsenow (Dispersed Flow Film Boiling, J. of Heat transfer, p.399, November 1968) cited the two-step process - heat transfer from wall to superheated steam and then from the superheated steam to liquid droplets - proposed by Laverty. The reality is that there are several direct and indirect processes

governing the heat transfer from the wall to the vapor and liquid in the dispersed film boiling and there is no accurate information to determine which portion of the heat transfer in the end goes to which particular phase. Therefore, accurate calculation of steam temperature may not be possible with present knowledge of wall to fluid heat transfer.

The uncertainty in the steam temperature calculation does not necessarily lead to a non-conservative impact on PCT. The key factors are total heat flux from the wall to the fluid and the liquid fraction in the dispersed film boiling flow. The steam temperature, which depends on the assumption of indirect heat transfer processes, is of secondary importance. Of primary importance is to model reasonably well the two key factors. It is concluded, from the inspection of all reflood assessments, that the combined effects of the interphase friction model, vapor generation (or interphase heat transfer) model, heat transfer model and conservative upper tie plate CCFL model, produce higher clad temperatures compared to data in the upper core region (from around 6 to 10 ft) where the PCT occurs and thus, have a conservative impact on PCT.

Question 71d: *Upper Plenum Entrainment/De-entrainment. Please discuss the manner in which de-entrainment in the upper plenum is calculated. Is there a model for de-entrainment on structures? How is entrainment to the hot legs and steam generator calculated? It should be shown that the S-RELAP5 over prediction of liquid buildup in the upper plenum is not due to under-prediction of entrainment to the hot legs and steam generators. Also since the code allows a second top down quench, does counter-current flow in any of the SETs, integral tests, and plant calculations reduce the clad temperatures or affect clad oxidation in the top of the core?*

Response 71d: There is no specific model for de-entrainment of liquid from any reactor component. In vertical components, a co-current (upward) flow solution implies entrainment of liquid and a counter-current flow solution implies de-entrainment of liquid. Among the various force terms in the momentum equations, the interphase friction is the primary factor in determining the flow directions between the two phases. Thus, liquid entrainment/de-entrainment is primarily a function of the interphase friction model. However, at the upper tie plate and steam generator inlet plenum junctions, a CCFL model is applied to limit the liquid down flow; therefore, entrainment/de-entrainment of liquid in the upper plenum is also affected by the CCFL model.

As discussed in Section 3.2.3, particularly, Equation (3.62), of EMF-2100(P) Revision 4, the interphase friction for the upper plenum component is enhanced to increase the liquid entrainment. Also, bounding values of CCFL input are used to hinder the liquid down flow to the core (see Response to Question 65 and discussion below). These two things insure that the down flow of liquid from upper plenum to core is conservatively calculated. The assessment of CCTF tests indicates that the top down quench range is much shorter than the data. Response to Question 122 presents a figure showing that there is no liquid down flow at the upper tie plate junction above the hot assembly.

On page 4-43 of EMF-2103, there is a discussion concerning the effects of CCFL input on the results from UPTF Test 29. The plotted results were not included in EMF-2103, but can be found in Figures 3.7.124 through 3.7.128 on pages 3.7-191 through 3.7-195 in EMF-2102. Those figures show that liquid hold-up in the upper plenum, as well as carry-over to the steam generators, varies with CCFL prediction. Since bounding values of CCFL input are used in the plant models, similar results are expected.

Question 71e: CCFL. *There are no special drag models in the downcomer specifically designed to treat countercurrent flow. Without these comparisons, there is no assurance that the CCF limit will not be violated during a plant calculation. Comparisons to countercurrent flow data would demonstrate that the liquid down flows in the downcomer do not violate CCFL. Figs. 4.116 and 4.117 show that the CCFL model is limiting the liquid downflow for many of the test points. This suggests the drag model tends to produce too high a liquid down flow for a given steam flow. Unless the drag model is different in the downcomer, these results suggest that the drag model will produce excessive liquid down flows in the downcomer. Please discuss the omission of the CCFL model or drag model specifically designed to model CCF in the downcomer.*

Response 71e: (See response to Question 65)

Question 71f: CCFL. *Since the S-RELAP5 code does not use a CCF limit model, interfacial and wall drag modeling is key to predicting CCF. Application of concurrent up-flow correlations for interfacial and wall friction to countercurrent flow tend to over-estimate the downflow of liquid. It appears that wall shear is neglected during countercurrent flow which would produce over-estimated liquid downflows in the low gas velocity region. Wall shear stress acting on falling water is almost the same order of magnitude as interfacial shear stress, making it inappropriate to ignore this stress. Since RELAP5 ignores wall shear during annular flow and EMF-2100 Section 3.0 did not show the details of the wall shear, discussion is needed that describes how wall shear is computed during CCF. This discussion should also compare the friction factor with data and show the behavior at low velocities/Reynolds numbers.*

Response 71f: S-RELAP5 does not ignore the wall shear under counter-current flow conditions and during annular flow. The description of S-RELAP5 wall friction is presented in Section 3.5 of EMF-2100(P) Revision 4. Unless the user purposely turns off the wall friction via input options, the wall friction is always evaluated under all flow conditions. (See response to Question 23).

Question 71g: CCF. *How is CCF modeled in the 2-D downcomer and how are the flow regime maps applied in this region?*

Response 71g: (see response to Question 65)

Question 71h: Hot Leg Entrainment. *Hot leg entrainment is underpredicted in Figs. 4.165-4.167, 4.173, 4.177, and 4.179, and, thereby it is not supported that hot leg entrainment is calculated conservatively. In some cases entrainment is not predicted until late in the test. Does the underprediction lead to a beneficial effect on PCT for the tests which offsets another conservatism elsewhere in the methodology? Fig. 4.173 shows no entrainment was calculated for the entire test. If the entrainment is calculated to match the data late in the test, this does not the model being conservative as stated on page 4-90 of EMF-2103.*

Response 71h: First, the assessment of the conservatism of carryover calculations was based on the accumulated results from three sets of tests. The carryover was dramatically over-predicted in full-scale, UPTF tests. The comparison in EMF-2103 Revision 0 Figures 4.164-4.167 are to levels in a catch tank downstream of the steam generator in the broken loop. Steam and liquid exiting the broken hot leg enter a separator at the top of this catch tank and the liquid is dropped into the tank. The level measurement is quite noisy – the plots have been smoothed significantly. In most cases, the measured level even indicates a level reduction in the early part of the transient. The measured values have a significant amount of uncertainty. In addition, the flow exited from the steam generator and traveled through fairly long pipes that

were modeled as having adiabatic boundaries. Heat transfer to the liquid on the secondary side of the steam generator and in the piping also contributed to additional uncertainties. As with the FLECHT-SEASET data, S-RELAP5 tended to under-predict the carryover when the rates were very low and to over-predict when they got higher. Test 54 (Figure 4.164) had somewhat higher flow rates than did Tests 62 and 68 and it was used to set the scaling factor for the interphasic drag at the inlet to the steam generator tubes. Test 68 also had high calculated carryover, although the data showed only a very small level change. Making a precise statement about the carryover calculations for these four tests is somewhat difficult and the adjustment of the drag was based on a comparison to test 54.

In Figures 4.168-4.171, the levels in the catch tanks downstream of the steam generator simulators were compared to calculated values for the full-scale facility, UPTF. For these tests, the carryover in the broken legs and in the intact legs was measured. Using the enhanced interfacial drag determined by CCTF test 54 resulted in a conservative prediction for the broken and intact legs. Using a nominal value of drag caused a slight under-prediction of levels in certain cases.

Figures 4.172-4.179 compare the levels in the separator tank and in the drain for the separator tank. The carryover is the sum of the two amounts. Test 31805 had very small carryover flows (the level in the separator didn't change and the level change in the drain tank was only about 2"), but Test 31203 had a more substantial amount of carryover and S-RELAP5 over-predicted the levels as long as the carryover was large. During the period from 150 seconds to 350 seconds, there was carryover, but it was not sufficient to show up as a level change in the main tank. Similarly, for Test 31302, S-RELAP5 under-predicted the carryover for low carryover rates. Once the flow became appreciable (~120 seconds), the calculated carryover was significantly higher than the measured. In this case, the modeling of the flow from the separator tank to the separator drain tank affects the filling of the drain tank at 130 seconds. A CCFL model was used in the drain and it held up the water flow to the drainage tank far more than the data would indicate. Removing the CCFL limit would result in a better fit to the level in the drain tank after 130 seconds, but the period before with the low carryover rates would still be under-predicted. Essentially the same comments apply to test 31701, except for the timing. There is a spurious level change in the drain tank when the operators intervened.

Overall, the conclusion reached was that for very low carryover rates, S-RELAP5 under-predicted the carryover. Once carryover became significant, particularly for the issue of steam binding in the steam generator, S-RELAP5 over-predicted the carryover. The under-prediction when carryover was very small was considered to be far less significant than the over-prediction during high carryover. The tendency of S-RELAP5 to over-predict in the strong steam-binding region was the basis for concluding that the modeling was conservative.

Question 71i: Two-Phase Pump Model. *The pump resistance and broken cold leg nozzle typically represent the largest resistances in the loop which determines the core flow (and hence fuel stored energy/PCT) during blowdown. It should be shown how the uncertainty in the relative resistances between the core and break through the downcomer and hot leg paths are taken into account and that the pump resistance, broken nozzle resistance, and the other loop resistances conservatively bound the expected variation (or are insignificant) in these path resistances from the core to the break.*

Question 71j: *Pump Differential Pressure Loss. How is the pump coastdown verified in the case there is no plant data? What is done in the modeling to assure the coast down is bounded?*

Response 71i & 71j: As stated in RAI response #24, the pump model is treated as best-estimate. This is necessary since control systems applied to pump speed (coupled with control systems on steam generator feedwater flow) are used to steady-state the plant model prior to a transient calculation. Without a reasonably accurate pump definition, code prediction of plant steady-state conditions will not agree with measured plant conditions. The figure-of-merit for pump performance is based on agreement of key steady-state operation variables including loop temperatures, flow rates, and pump speed.

Pump coastdown is not explicitly addressed in this methodology's PIRT given in Table 3.4 of the methodology document. As may be inferred from the PIRT, the two-phase pump degradation was ranked as having a strong phenomenological impact on PCT during blowdown, while the pump differential pressure loss has a strong impact on PCT during reflood. However, in the sensitivity study shown in Appendix B.4, the PCT impact of two-phase pump degradation was much less than anticipated by the PIRT team. During reflood, S-RELAP5 evaluates the pump differential pressure loss directly from the single-phase pump performance characteristics required in the pump model. Pump seizure is not considered part of a best-estimate LBLOCA scenario; and, for this reason, it is not considered in this methodology.

Pump performance (including pump differential pressure loss) during single-phase conditions is based on best-estimate pump-specific performance data. It has been Framatome's experience that most plants have this single-phase pump data available for modeling purposes and usually have pump coastdown data for model benchmarking. Large disparities from actual and calculated pump characteristics are unlikely since the steady-state simulation would fail to show loop temperatures and flow rates consistent with plant data. The CE/EPRI two-phase pump degradation model will be used in the RLBLOCA methodology and the methodology document, EMF-2103, will be revised to indicate this (see Appendix D).

As stated in RAI response #24 and #35, the uncertainty in the broken nozzle k-factor and the relative resistances from the core to the two ends of the break is a break flow/flow split issue.
[

]

Question 71k: *Non-Condensable Transport. The Achilles Test # 25 under-predicted the PCT later in the event. While the effect of the nitrogen is to initially force additional water onto the core providing some early limited core cooling, the later overall effect is to reduce core cooling since the higher initial steaming reduces the liquid inventory in the core causing a late heat-up of the core. S-RELAP5 under-predicted the negative effects while capturing some of the early beneficial effects. Please discuss the basis for including the early beneficial effects of nitrogen in plant calculations and not considering this parameter in the uncertainty methodology and imposing it as a penalty on PCT.*

Response 71k: The Achilles test (ISP #25) simulation was performed to confirm the ability of S-RELAP5 and the RLBLOCA methodology (including modeling assumptions) to simulate the effects of nitrogen injection on core cooling following the emptying of the accumulators. The test assembly consisted of an array of rods, arranged in a Cartesian x-y grid, inserted in a cylindrical pipe. This resulted in an extremely large degree of radial and azimuthal inhomogeneity in the fuel rod flow areas. For the outside rows of rods, there were fairly significant gaps where the Cartesian rod array could not be forced to match the round tube. As a result, many of the rods near these gaps quenched very quickly. See the temperature traces in Figure 3.15.5 of EMF-2102. It was apparent that water was coming up the bundle through these gaps and quenching at fairly high elevations very quickly. An accurate modeling of the gaps between the fuel rods and the pipe would have been required to predict temperatures accurately. The degree of inhomogeneity far exceeds that present in a PWR core and the model would have had to differ fairly significantly from the core model to be used in the methodology. By adjusting the model carefully it would have been possible to get a better fit to later PCTs, but the comparison would not have used the core model appropriate for the methodology. Therefore, an accurate model was not created.

For the approximate model based on the methodology, the core was broken into two areas and the flow areas and flow resistances were adjusted to account for the very large by-pass areas in the outer portion of the core in an approximate way. Two different groups of rods were considered: those on the inside area and those on the periphery. The flow areas for the rods on the periphery were adjusted to account for the open flow area and the flow resistance was reduced to account for the open flow paths on the periphery. Given the model simplifications of a very complicated flow pattern in the test assembly, the under-prediction of the PCT at the PCT node is not particularly meaningful. If one refers to Figures 3.15.12 through 3.15.17 of EMF-2102, the PCT elevation is the elevation where the predicted temperature falls below the measured. For the neighboring measurements (within about 8"-10" of the PCT elevation), S-RELAP5 over-predicts the temperatures. In addition, note that the temperatures show far less variability at the other elevations than is seen at the PCT elevation (with the possible exception of the temperatures at 3.18 m). Thus, some fairly complicated three-dimensional flow effects that would not be modeled in a LBLOCA are determining the PCT for this test.

Considering the approximate nature of the modeling for the fuel rod array, a reasonable agreement between the calculated PCT and the measurements was deemed sufficient for the evaluation of S-RELAP5.

With this test, the trade-off of early cooling and late heating is fairly obvious. One can force the nitrogen to go through the core by increasing the resistance in its alternate flow path. The effect is a quick flushing of all of the liquid in the downcomer and "lower plenum" as well as the core. This results in a rapid cool-down of the fuel rods. When the initial surge of cooling is past, the liquid inventory is nearly gone from the region below the core and the rods begin an adiabatic heat-up until the liquid finally fills the "lower plenum" region and enters the core. This results in a more rapid heat-up until the liquid reaches the core again, after which the heat-up is in pretty good agreement with the data. However, the fast heat-up more than offsets the initial cooldown and results in a slightly higher PCT than was observed. For a LBLOCA, one does not experience this range of variability in the modeling. The amount of early cool-down in ISP #25 was just a consequence of adjusting the resistance in the escape path for the nitrogen so that it would match the rate of escape of the nitrogen.

[

] The effect of the nitrogen injection can be seen in the core level plot (Figure 5.27) and on the fuel rod temperature plot (Figure 5.18) for the sample case shown in EMF-2103. There is clearly an effect on the temperatures when the nitrogen enters the system. It has been shown in the analysis of Achilles ISP #25 that S-RELAP5 under-predicts any initial beneficial effects of the nitrogen on the PCT. Since S-RELAP5 is conservative with regard to this aspect of nitrogen injection and since it generally over-predicts temperatures in the test assembly, with the exception of the PCT elevation, which has large variability in the measured temperatures; there is no need for a penalty.

Question 711: *Downcomer Entrainment. Please identify the correct section in Ref. 5 for the downcomer entrainment tests and discussion referred to in Section 4.3.3.1.10 of EMF-2103. Please discuss the cause of the lower plenum liquid level oscillations in Figs. 4.106 through 4.110, including the flow regimes predicted by S-RELAP5 during this period, and the steam and liquid velocities in the downcomer and exiting the lower plenum during these tests. Does the under-prediction of the liquid inventory in the lower plenum enhance the steam downflow in the core during blowdown and produce a beneficial effect on PCT? Does boiling occur in the lower downcomer and lower plenum in these tests and what effect does boiling versus no boiling have on the entrainment?*

Response 711: The reference indicated in EMF-2103 is correct. The reference is "Section 4.3.1 and Reference 5" where the section referred to is in EMF-2103. In Reference 5 the section of interest is Section 3.7.4.

The lower plenum liquid level oscillations are described in Section 3.7.4.4.1 and the steam and liquid mass flows are provided in Table 3.7.5 of EMF-2102, Revision 0. There were also two sensitivity studies performed to look at these oscillations and they are reported in Section 3.7.4.4 of EMF-2102, Revision 0. The first sensitivity study looked at turning off the mixture level model in the lower plenum and the second sensitivity study looked at using a 2D component in the lower plenum. With the mixture level turned off the oscillations were significantly reduced but the lower plenum liquid level was in worse agreement with the data and even more conservative. With the use of a 2D component in the lower plenum, the comparison to data was significantly improved. However, there was a new set of oscillations in the predictions relative to the data. An undocumented calculation was also performed to look at the use of the 2D lower plenum model in the sample plant calculation. This calculation indicated that the 2D lower plenum model provided a less conservative PCT but significantly increased the run time. Based on this evaluation it was decided to go forward with the lower plenum model reported in EMF-2103, Revision 0.

With respect to the possibility of enhanced steam down flow in the core with a potential benefit on PCT, a lower liquid level in the lower plenum would tend to amplify this possibility. However, this effect, if it did occur, would have a secondary influence on the PCT relative to the delay in the initiation of reflood. The increase in predicted bypass flow and associated decrease in lower plenum fill rate has a direct impact on the predicted PCT. The overall conservatism of the methodology (code and nodalization) is clearly demonstrated in the conservative PCT's calculated for both the LOFT and Semiscale integral assessments.

Very little if any boiling would have occurred in these tests. The tests were conducted by first bringing the system temperature up to that of the steam temperature and then initiating the flow

of the ECCS water. The tests were specifically designed to look at downcomer and bypass flow versus steam flow up the downcomer. The expected impact of boiling in the downcomer in these tests would be to further impede the liquid flow down the downcomer and to increase the bypass flow.

Question 71m: *Downcomer Level Oscillations.* Fig. 3.11.47 of EMF-2102, shows large oscillations in void fraction. Please discuss the model conservatism as stated in Section 4.3.3.1.11, since the core in these tests shows large void oscillations which can "provide additional core cooling" as pointed out on page 4-92. If downcomer boiling occurs during accumulator discharge, what is the effect on PCT after the accumulators empty.

Response 71m: The indicated figure does show large oscillations in the core void fraction. However, the figure also shows that while the code does under predict the void fraction for short periods of time during these oscillations, on average the code conservatively over predicts the void fraction relative to the measured data. This general over prediction of the core void fraction will lead to the prediction of higher conservative PCTs. This conservatism is clearly shown by the over prediction of the temperatures demonstrated in Figures 3.11.36 through 3.11.45.

In general, the impact of downcomer boiling is to delay the flow of water down the downcomer and into the lower plenum. Given this, if downcomer boiling occurs during accumulator discharge the impact would likely be an increase in the amount of accumulator water that would bypass the core and be lost out the break. Given the loss of additional accumulator water, the PCTs would be expected to increase.

Question 71o: *Lower Plenum Sweepout.* Oscillations suggest that the sweep out of the liquid from the lower plenum is retained in the downcomer and immediately flows back into the lower plenum periodically. In such a case, please discuss the model conservatism regarding the lower plenum liquid level test predictions. Should there be flow of liquid back into the lower plenum, does this result in entrained liquid entering the core and providing additional cooling? Discuss the need for bias in the uncertainty evaluations if the lower plenum oscillations cool the core.

Response 71o: The UPTF ECC penetration tests were designed to simulate ECC flow in the downcomer during the LBLOCA blowdown-refill period when the accumulator ECC water penetrates the downcomer and the steam flows down the core and up the downcomer to carry out the water to the break. Under such circumstances, steam flow is in the wrong direction to entrain water to the core. Furthermore, a very strong steam flow is required to produce such large oscillations. For a cold leg break with pump off, the steam flow from the lower plenum to the core, if present, can never be strong enough to produce lower plenum level oscillations of significant amplitudes. Accordingly, the situation of large lower plenum oscillations enhancing liquid entrainment to the core does not exist and is not calculated to occur in plant applications; therefore, there is no need to evaluate the bias or uncertainty for such an event that either does not exist or is of no significance.

It should be pointed out that the large lower plenum oscillations are due to the conditions peculiar to the UPTF Test 6 series and are not observed in plant applications. As discussed in Section 3.7.4.4.1 of EMF-2102(P) Revision 0, the large oscillations go away if the mixture level model is turned off in the bottom volume of the lower plenum. With reference to the nodalization showing in Figure 3.7.4 of EMF-2102(P) Revision 0, the conditions for improper appearing and disappearing of mixture level (more precisely liquid level) in the bottom volume for the Test 6

series are: (1) the lower plenum is initially empty, and (2) no significant amount of steam flows to the bottom volume and the liquid drains slowly to the bottom; therefore, the fluid velocities in the bottom volume are low. These conditions are not present in the plant calculations, since the lower plenum is initially full of water and the void fraction difference between the two lower levels is never large enough to produce a liquid level in the bottom volume.

Therefore, in plant calculations, the lower plenum sweep-out behaves like those shown in Figures 3.7.38, 3.7.41, 3.7.44, 3.7.47 and 3.7.50 of EMF-2102(P) Revision 0. Thus, all liquid above a certain level, which depends on the vapor velocity, of the upper lower plenum volume is carried out of the lower plenum by the vapor, and large oscillations are not present. Note that if the lower plenum is nodalized with more axial levels and with a narrow upper flow path to allow vapor to flow through the lower plenum without much liquid entrainment, no significant sweep-out will occur. The results will be similar to those obtained with the 2-D horizontal component discussed in Section 3.7.4.4.2 of EMF-2102(P) Revision 0. The present two axial level 1-D lower plenum nodalization is a necessary compromise to satisfy certain steady-state requirements. With such a nodalization, conservative lower plenum sweep-out is calculated. However, the sweep-out does not lead to liquid entrainment into the core since the vapor flow either is in the wrong direction or is not strong enough to cause significant entrainment.

Uncertainty Analysis

Ref: EMF - 2102(P)

Question 72: 5.1.1 Data Set Adequacy

With regard to Table 5.1 it appears that not only the maximum pressure data, but also the mass flux of the vapor and liquid do not bound the intended application. Please justify in greater detail your statement that the data set on which film boiling multipliers, bias, and uncertainty are determined adequately cover the intended application.

Response 72: [

]

Question 73 (Part 1): 5.1.2 Inferring Heat Transfer Coefficients from Experimental Data

Please describe mathematically the inverse conduction algorithm (flow diagram and a few equations) used in computing the boiling heat transfer coefficient from the thermocouple data.

Response 73 (Part 1): The requested material is provided (see Appendix A).

Question 73 (Part 2): *In Fig. 5.1 is this the numerical node scheme for the inverse algorithm? If so, at what node is the thermocouple?*

Response 73 (Part 2): In Figure 5.1, the thermocouple is at the boundary between the boron nitride and the clad inside surface.

Question 73 (Part 3): *Specifically, how is the surface heat flux a function of the derivative with respect to time, as stated in sec. 5.1.2.1?*

Response 73 (Part 3): The transient heat conduction equation (one-dimensional, cylindrical geometry) is solved to determine the heat flux at the clad surface.

$$\rho c_p \frac{\partial T}{\partial t} = \frac{1}{r} \frac{\partial}{\partial r} \left(kr \frac{\partial T}{\partial r} \right) + q''$$

The first term in this equation contains the temporal derivative. The term in parenthesis, when divided by the area, is the heat flux. Thus, the heat flux will vary with time.

Question 73 (Part 4): *The thermocouple measures the temperature $T(r_0, z_0, t)$ (i.e. at some fixed point (r_0, z_0) as a function of time t (as in Figs. 5.2 and 5.3). The objective seems to be to compute the surface temperature at the same elevation at the same time points as the thermocouple measurements. So where is the time derivative necessary? Where is the source of the amplification?*

Response 73 (Part 4): The time derivative is necessary to capture the effects of stored energy in the electrically heated rod during the transient test. Failure to include this term will cause the derived convective heat transfer coefficients to have a bias that is related to the lag of the transfer of stored energy to the coolant.

The experimental measurement is of temperature. These measurements are taken discretely, at intervals that are on the order of 0.5 second (FLECHT-SEASET). To obtain the heat transfer coefficient, the heat flux must be inferred (calculated) from these temperature measurements. The heat flux is a function of the derivative of the temperature, which, mathematically, is the slope. The slope is quite small in magnitude so slight variations in the temperature will cause apparently large variations in the heat flux.

Question 74: 5.1.2.1 Signal Filtering

Question 74 (Part 1) *What is the t between thermocouple signals?*

Response 74 (Part 1): FLECHT-SEASET Tests: 0 to 200 seconds (0.5 sec between samples); after 200 seconds (1.0 sec between samples).

Question 74 (Part 2): *What is the thermocouple instrument error?*

Response 74 (Part 2): The 2-sigma uncertainty of rod sheath thermocouples in THTF is reported by the experimenters to be 10.3 K. An additional 0.3 K is added to this to obtain the nominal transient uncertainty, applicable except at the time of quench.

For FLECHT-SEASET, the thermocouple instrument error is 3/8% of reading between 277 C and 1316 C. This is combined with a conditioner error of $\pm 1.01^\circ\text{C}$ and a readout error of $\pm 2.03^\circ\text{C}$.

Question 74 (Part 3): *The thermocouple reading has two sources of variation:*

i) the instrument error

ii) a variance due to the fluctuations in the underlying physical process. (If we had a perfect instrument, this variance would still be there.)

Do you estimate these effects?

Response 74 (Part 3): Fluctuations in the underlying process were treated qualitatively by filtering the data. Of primary interest is the modeling of the limiting hot rod and the conditions surrounding it. Test data associated with rods within 2 rows of the shroud (channel wall) were removed from consideration because they exhibit cold wall effects that would skew the results.

Question 74 (Part 4): *What is your stopping rule with regard to smoothing of the thermocouple readings with respect to the above variances?*

Response 74 (Part 4): The above variances were not used to establish an acceptance criteria for smoothing the thermocouple readings. The thermocouple data were filtered first with the median filter, then with the binomial filter.

Question 74 (Part 5): *What is your stopping rule with regard to smoothing the inferred heat transfer coefficients (as in Figs. 5.4 and 5.5)?*

Response 74 (Part 5): The above variances were not used to establish an acceptance criteria for smoothing the heat transfer coefficients. The heat transfer coefficient data were filtered first with the median filter, then with the binomial filter.

Question 74 (Part 6): *Do you apply any quantitative measure to claim that "the underlying features of the signal are intact"?*

Response 74 (Part 6): No. This was performed visually by examining sample thermocouple signals processed by the algorithm. As a check that the procedure works acceptably, the results were compared with qualified published results, a sample of which is shown in Figure 5.6.

Question 74 (Part 7): *Comment: Fig. 5.6 is irrelevant.*

Response 74 (Part 7): Agreed, it may not be necessary to retain this figure in EMF-2102.

Question 75 (Part 1): *5.1.3 Data Consistency Check*

Question 75 (Part 1): *Since the test data provide multiple estimates of HTC for common times and elevations, is the mean computed at some specific time and elevation the "truth" with respect to which you compute the bias in the computed value at that time and elevation; and the standard deviation the uncertainty?*

Response 75 (Part 1): We take the values which remain after evaluation of the data and average them. The purpose of the averaging is to obtain a value comparable to the calculated value from S-RELAP5 that represents a nodal volume average.

Question 75 (Part 2): *How do you assure that the data were not oversmoothed? (That is only the instrument error and outliers were removed.)*

Response 75 (Part 2): Smoothing does not necessarily remove the instrument error. It does, however, help remove a part of the truncation error that is part of the analog to digital conversion (this causes the flat spots of apparent zero slope). In THTF, the smoothing of the median filter also removed the sharp temperature spikes that occurred in the data (the experimenters attributed this non-physical behavior to the power supply). Because the same smoothed data was used for analysis of T_{min} and quench time (described in Appendix B), and excess smoothing would round the "knee" in the thermocouple trace, minimal smoothing was applied to the data. The largest effect of smoothing occurs near quench and this effect is discussed in Appendix B to these RAIs.

Question 76: *5.1.4 Partitioning the Data*

The data are partitioned into two sets. What are you validating? Are the THTF and FLECHT - SEASET data considered initially as one set and then split into two through random selection?

Response 76: The data that we have are sampled from the population of possible values. In order to ensure that our result (the curve fit) applies to the population as a whole, and not just to the sample, we divide the sample randomly into two parts. One part is used to develop the curve fit (the multipliers). The other part serves as a check that our curve fit applies more generally to the population.

Question 77: *5.1.5 S-RELAP5 Calculated HTC*

5.1.5.1 Data Averaging

The oscillations in the computed values of void fraction, heat transfer coefficient and clad temperature are attributed to changes in the heat transfer mode in the course of the computation (i.e. film boiling, single-phase vapor)

Question 77i: *What is the variable and its value that determines which mode to assume?*

Response 77i: The S-RELAP5 variable is RFLMOD. The value is the same as for variable HTMODE described in EMF-CC-097 in Section 4.5. Film boiling is identified by HTMODE=7. Single-phase steam is identified by HTMODE=9.

Question 77ii: *What is the time increment in the computation and what is the average cycle length of the oscillation in the void fraction, and T_{clad} ?*

Response 77ii: The S-RELAP5 time step is dynamically determined during the course of the transient to satisfy numeric stability requirements. The maximum allowable time step is input by the user. The user also determines the frequency of writing data to the plot file. This frequency was chosen to correspond to the smallest time step in the measured data. For FLECHT-SEASET, the time increment in the plot file is 0.5 seconds. For THTF, the time increment in the plot file is 0.05 seconds. An analytical computation of the average cycle length in the oscillations in the code was not computed. The cycle length changes as the transient evolves, but is about 2 to 6 seconds per cycle prior to the time of quench.

Question 78a (Part 1):

Is it correct that RELAP computes the void fraction (α), the heat transfer coefficient (h) and the clad temperature (T_{clad}) sequentially as follows:

$$\alpha - h = T_{clad}$$

Response 78a (Part 1): No. The calculation is $h \rightarrow T_{clad} \rightarrow \alpha$.

Question 78a (Part 2): *If so, is the same algorithm applied with the 8 sec. window? How does the window size compare to the computational time step?*

Response 78a (Part 2): Yes, the same algorithm is applied with the 8 sec window. The window size is larger than the calculation time step.

Question 78a (Part 3): *How does it compare to the time step in the T_{clad} measured values?*

Response 78a (Part 3): The window size is larger than the Δt between measured values of temperature.

Question 78b (Part 1): *Is the following sequence of computations during processing of the data correct?*

Let $D(t)$ be the original values at time t . Assume $w = 3$. Then

$$\bar{f}_3(4) = (1/3) (D(1) + D(2) + D(3) + D(4))$$

$$\bar{f}_3(5) = (1/3) (D(2) + D(3) + D(4) + D(5))$$

etc.

Then $f_{smooth}(t-w/2) \leftarrow f_w(t)$ for each $t \geq w/2$.

Response 78b (Part 1): The description of the averaging of the described S-RELAP5 values is the following:

A running average is used to smooth the S-RELAP5 calculated data. It is applied to the void fraction, the clad surface temperature, and the heat transfer coefficient. Through use of control variables it is possible for S-RELAP5 to compute a running average. Part of this running average is computed with S-RELAP5 control variables. The final construction of the running average is performed by post-processing. The S-RELAP5 integrating component computes:

$$I(t) = \int_0^t f(t) dt$$

In S-RELAP5, a delay component may be used to save results of the integration for states that occurred w seconds in the past. Effectively,

$$I(t-w) = \int_0^{t-w} f(t) dt$$

The running average is obtained by taking the difference between these two equations and dividing by the difference in time.

$$\bar{f}_w(t) = \frac{1}{w} [I(t) - I(t-w)] = \frac{1}{w} \left[\int_{t-w}^t f(t) dt \right]$$

The running average generated by this algorithm is a "trailing" average. That is, the average lags the physical behavior. During post-processing of the data, each of the running averages is further refined to generate a central running average. The changes made are:

- Shift the averaged data to the left by $\frac{1}{2}$ of the window width w . This is effectively accomplished by discarding the first half of a windows width of averaged data.
- Second, do not average over the quench front. Therefore, from the quench time less a window width, replace averaged data with raw data.
- Third, patch the first part of the running average by using raw data instead of averaged data. This is necessary because the delay component results in averaging of zeros until the time reaches the window width. The window width, w , is 8 seconds.

Question 78b (Part 2): *Is it correct to say that you compute a moving average with a lag of w and then shift the value back by $w/2$ in time?*

Response 78b (Part 2): S-RELAP5, with the use of control variables, is able to compute a moving average that is based on the recorded data over the previous w seconds. For a function $f(t)$, this average, $f(t)_{avg}$, lags the actual system behavior $f(t)$. This average can be translated into a central average by shifting the time scale by $w/2$ so that half of the interval is in the past, and half of the interval is in the future. On this basis, the answer to the question is yes.

Question 79: *In reference to the comparison shown in Figs. 5.18 through 5.20.*

Question 79a: *Are you applying the same algorithm (i.e. w) in the vapor and quench parts of the curves as in the transition region?*

Response 79a: The algorithm is being applied to the vapor parts but not to the quenched parts. Treatment near the quench front was described in another response above.

Question 79b: *How would enlarging the window result in larger segments of unsmoothed data in the film boiling regime?*

Response 79b: Under some conditions, the inverted annular flow regime (associated with FILMBL) is very short, only a few inches in length. To avoid imparting a bias that includes nucleate boiling (high heat transfer coefficients) that occur at the quench front, it is important that averaging not be applied across the quench front. The calculated data that is within $w/2$ of the quench front is not averaged. A larger w would mean that more of the data is not averaged and more oscillations in the calculation that is to be compared to data. A larger window also results in more of the calculated data at the start of the transient not being smoothed, by width w .

Question 79c: *How is stopping the smoothing at the level where the amount of ripple remaining is on the order of what might be expected as experimental uncertainty relevant? The computation is deterministic, therefore, experimental uncertainty cannot be reproduced. By not smoothing "completely" how can you be sure you are not skewing the distribution on which your uncertainty estimate in the multiplier is based?*

Response 79c: When it was determined that smoothing was necessary, it was applied with the intent to use the minimal amount of smoothing necessary to provide a calculated value that would be comparable to a measured value.

Clearly, the fluctuations observed in the S-RELAP5 calculated void fraction and heat transfer coefficient are not observed physically and are artifacts of the code model. To not smooth would cause very large (and unacceptable) uncertainties.

On the other hand, smoothing causes curvature of gradients to be reduced. If the gradient is "real," then excess smoothing would introduce a bias in the results. Therefore, a compromise was struck. The smoothing, although essential, should be minimized, and consideration of experimental uncertainty was used only to establish a rough estimate for assessing if the amount of smoothing applied was adequate.

Question 79d: *Therefore, what harm is there in smoothing completely, in view of the comparisons shown in Figs. 5.18 through 5.20?*

Response 79d: Additional smoothing in this case would be acceptable.

Question 79e: *5.1.6 Multiplier Correlation*

You are determining two heat transfer coefficient correlation multipliers in this section

M_{FILMBL} and M_{FRHTC}

Correct?

M is a function of z (fuel height) and t the time in the transient, since $h_{meas}(z_0, t)$ and $h_{calc}(z, t)$, where z_0 is the thermocouple location. Correct?

Response 79e: It is correct that two heat transfer coefficient correlation multipliers are being defined.

It is possible for M to be a function of the elevation, as an artifact of experiment design. But the correlation and the multipliers are functions of local conditions and do not include the elevation as an explicit parameter.

Question 80: *How do you define quench front?*

Question 80i: *At a thermocouple location z_0 how do you determine the time of the quench front at that location from the measured data?*

Response 80i: The determination of quench in the measured data is based on the FLECHT-SEASET algorithm for the low pressure data. This algorithm was not directly applicable to the

high pressure test data in THTF. The higher sampling rate in THTF made it possible to devise an algorithm that uses the maximum negative curvature in the thermocouple trace (a mathematical way of finding the "knee" in the curve). The mathematical algorithms and description are presented in Appendix B to these RAIs.

Question 80ii: *How are M_{FILMBL} and M_{FRHTC} related to the definition of quench front?*

Response 80ii: The quench front identifies the boundary between nucleate boiling and film boiling in the test section and in the code calculation. The multipliers apply only to film boiling.

Question 80iii: *In aligning the quench fronts to a common location (say z_0), what parameters are you equating? (i.e. $P_{meas}(z_0, t_{meas}) = P_{calc}(z_0, t_{calc})$?)*

Response 80iii: The quench fronts identify a point of commonality between the calculation and the measurement. By using the quench front (instead of time) as the basis for comparison, the section of the heated length that is in nucleate boiling is common between the measurement and calculation and the section of the heated length that is in stable film boiling is common between the measurement and calculation. By aligning these features, the void fraction distribution as a function of elevation above the quench front should be comparable between the measurements and the calculation, and the axial pressure profile should also be close. This means the local conditions on which the film boiling heat transfer coefficient is based will also be closely similar between the measurement and the calculation.

Question 81 (Part 1): *You state "Temporal displacements between THTF measured data and code calculations were ignored. The transients are sufficiently short in duration that the temporal differences are expected to be small."*

In principle, is it not the relationship between the time step size in the transient calculation in relation to the temporal differences that is the issue, and not the duration of the transient? Please explain your reasoning in greater detail.

Response 81 (Part 1): The transient begins with virtually identical conditions between the measurements and the calculation. However, minor differences between the state of the calculation and the measurement will grow as the transient progresses. In a shorter transient, the differences are insignificant. For a longer transient, this will not necessarily be the case. For example, in a rod temperature plot from a long transient, the small differences in heat transfer rate cause the location of the peak clad temperature and the quench front to shift significantly. Many of the observed differences can be removed by applying a small temporal shift to the calculated data.

The heat transfer correlations are evaluated based on "local conditions." To obtain the best possible basis for comparison, the local conditions need to be comparable, with temporal differences removed. The results would be heavily skewed if, for example, the measured point of comparison was quenched and the calculated value was not quenched.

Question 81 (Part 2): *Note: Since*

$$M(t) = h_{meas}(t) / h_{calc}(t)$$

a misalignment of h_{meas} and h_{calc} with respect to time will introduce a bias in the distribution of $M(t)$ (which t will be used in $M(t)$, the one from the measurements or from the calculation?)

Response 81 (Part 2): M was not correlated to be a function of time. A value of M was chosen that applies independent of time. To remove the temporal differences in the FLECHT-SEASET data, the location of the quench front as a function of time was examined. Times were chosen that correspond to when the quench front was just below a differential pressure measurement location. This choice affects the measurement of the void fraction. The time associated with that measurement was used to obtain a snapshot of the measured data. Then, the S-RELAP5 calculation was examined. When the quench front reached the same location as that in the test, the time was noted and a snapshot of the calculated values was obtained. These were then compared directly to the measurements. Therefore, the expression above for M should be written

$$M = \frac{h_{meas} [t_{meas} (z_{quench})]}{h_{calc} [t_{calc} (z_{quench})]}$$

Question 82: *5.1.7 Film Boiling Multiplier Statistics*

5.1.7.1 Defining Data Set

Is this the same partitioned set as described in sec. 5.1.4?

Response 82: Yes.

Question 83: *I do not understand the first paragraph!*

Question 83i: *Does "multiplier pairs" mean M_{FILMBL} and M_{FRHTC} ?*

Response 83i: Yes.

Question 83ii: *How were $M_{FILMBL} = [\quad]$ and $M_{FRHTC} = [\quad]$ determined?*

Response 83ii: The multipliers were determined by trial and error. Values were chosen and code calculations performed. The calculated values were then compared to the measured values and the mean and standard deviation calculated. A mean of 1.0 corresponds to the desired solution.

Question 83iii: *What does "The correlating set had a mean of 1.00 and a standard deviation of 0.373." mean? In particular, what is the "correlating set"?*

Response 83iii: As explained, the data which has been collected in experiments represents a sample of the population. This sample was randomly divided into two parts. The first part, the defining data set, (used for correlation, hence the name correlating set) is used to determine the multipliers. The validating set is not used to develop the multipliers.

Question 84: *Please explain the rest of this section more clearly.*

Question 84i: *Figs 5.21 through 5.23 refer to frequencies of measured-to-calculated HTC ratios. what happened to the distinction between FILMBL and FRHTC?*

Response 84i: M_{FILMBL} and M_{FRHTC} were not independently determined. They were determined together, and are part of the code model. In the model, M_{FILMBL} is applied when the void fraction is less than []. M_{FRHTC} is applied when the void fraction is greater than []. Some combination of these two multipliers, as determined by the interpolating function, is applied between void fractions of [].

Because of the oscillatory behavior of the code heat transfer mode, and a transition region where both multipliers apply, an integral approach to the determination of film boiling heat transfer multipliers was required. The figure of merit on the fit is the ratio of the measured to calculated heat transfer coefficient. For both the inverted annular film boiling regime and the dispersed flow regime, this heat transfer coefficient ratio should have a value of 1.0. The interpolating region between the two regimes should also have a ratio whose value is 1.0. Therefore, this is what is reported, for all of the data.

Question 84ii: *Similarly, in the fit of M vs. α , what heat transfer regime is assumed and why?*

Response 84ii: The data has been filtered so only data which is in stable film boiling is considered. The curve fit of M vs. α considers all of the measured data - some of which is inverted annular film boiling, some of which is dispersed flow film boiling, and the remainder of which is in the transition between inverted annular and dispersed flow. The expression indicates that there is not a significant bias in the heat transfer coefficient ratio associated with either multiplier or the combination of the multipliers.

Question 85: *5.1.7.2 Validating Data Set*

Is it not true that both the correlating set and the validating set are random samples from the some data set? I fail to see what you are validating in that case.

Response 85: The collective set of test data represents a sample of the population. Each one of the points in the data set represents a sample from this population. In an ideal world, one would collect data by sampling the population and then develop a model which describes the population from the sample. Then, to demonstrate that the model applies to the population, additional data would be collected by sampling from the same population. This additional data is evaluated with the model to determine if the model provides an adequate simulation of the population. In our development, the ideal world does not exist because the data has already all been collected. So the process must be emulated. This is performed as follows.

Formal methods were applied to develop the multipliers (develop the correlation). Since all of the data was already collected, each of the data points were treated as a sample from the population. The samples were randomly divided into two parts. The first part, the correlating data set, was used to develop the multipliers. The validating data set was set aside, to be used later after the correlation development (the multipliers) is complete. The validating set is used to extend the applicability of the model to the population, which is more than the set of data that has been collected, separately or collectively.

Question 86: 5.1.7.3 Probability Distributions for Film Boiling

It seems to me that a lognormal distribution would be more appropriate for $f(x)$. There is no reason a priori to separate $f(x)$ into two terms based on low and high void fraction. Moreover a discontinuity in the derivative with respect to void fraction is introduced. Please explain.

Response 86: A log-normal distribution for $f(x)$ could be used. However, it doesn't fit the data as well. As a first step in selecting the appropriate empirical distribution for the data, two parameters were calculated based on the data:

$$\beta_1 \equiv \frac{\mu_3^2}{\mu_2^3}$$

and

$$\beta_2 \equiv \frac{\mu_4}{\mu_2^2}$$

where

$$\mu_n \equiv E[(x - \mu_1')^n]$$

These values, which depend on the skew and kurtosis of the distribution, were then plotted on a chart (see for example, Figure 6.1 of "Statistical Models in Engineering," Gerald J. Hahn and Samuel S. Shapiro, John Wiley & Sons, 1967) which was marked into various regions in which different types of empirical distributions were best choices.

The calculated values of the parameters clearly excluded the Log-normal distribution, the Normal distribution and the Gamma distribution. The Log-normal is excluded because the data show a much lower value of β_2 , corresponding to greater peakedness. The Normal distribution was excluded based on the amount of skew. The Gamma distribution was excluded because the skew was too small for the kurtosis. The best candidate was a Beta distribution, with the preferred choice of parameters corresponding to a J-shaped distribution. This distribution is a simple polynomial form, applying over a range of the parameter. The only problem with a reverse J-shaped Beta distribution is that it goes to infinity as the argument goes to zero. The distribution chosen was a simple polynomial form, applied to a finite range of the variable, and it was designed to bound the probability distribution, fit the probability density as well as possible and provide a simple algorithm for use in the Monte Carlo calculations.

By changing the functional form at the peak, a discontinuity in the derivative of the probability density is introduced. However, there is no reason to avoid a discontinuity in the derivative of a probability density or distribution. These occur all the time. In fact, discontinuities in the distribution itself are not uncommon. The only requirements of a probability density function are that it be positive definite and that the integral from negative ∞ to positive ∞ be unity.

Ref: EMF - 2103(P) Rev. 0

Question 87: 4.3.4 Evaluation of Code Biases

In the first paragraph you state that "..., the evaluation of the biases does not include uncertainties."

The biases do have uncertainties associated with them as you have quantified in Table 4.19. In order to make the conclusion in section 4.3.4.4 "The application of the biases resulted in a reduction in the maximum PCT predicted by the code,". Therefore, the bias corrected value of the code is a prediction. This in my view requires that the uncertainty in the bias be taken into account. Please explain.

Response 87: The evaluation of the impact of the calculated biases for the code was based on the mean values of the biases and did not include the uncertainties. This was done for two reasons: the first was that inclusion of the uncertainties would have necessitated a statistical analysis of each of the tests; and second, having done a couple of the LOFT tests statistically, it was found that making the comparison to data was a little more difficult.

The comparison of the code predictions to the data, using a statistical analysis results in a family of predicted cladding temperatures. Many of these predicted temperatures fall above the data. Many are below the data. Thus, the result of considering the uncertainties is a band of predicted temperatures that encompass the assessment data. It can be concluded from these comparisons that there is enough uncertainty in the calculational model to bound the data, high or low, but it does not provide a clear indication of the impact of removing the code model biases.

When the calculation is based on only the mean values of the biases, it can be seen that the biases determined in the separate effects tests have not degraded the ability of the code to predict integrated tests. This point is important in that values inferred from a set of small-scale, separate-effects tests do not a priori have to result in anything meaningful for larger-scale integral-effects tests. If the model is applicable and scalable, the biases will be meaningful for the large scale tests. Thus, comparing the code prediction with the model biases removed to the data supports the bias determination and the scalability of S-RELAP5. The fact that in virtually all cases, the predicted values improved when the model biases were removed provides even more support for the applicability and scalability of the S-RELAP5 code.

Question 88: 4.4 Determination of Effect on Scale (CASU Step 10)

Please comment on the following argument and how your conclusions with regard to the ability of S-Relap5 to scale the requisite phenomena with regard to a RLBLOCA are valid in this context.

A Heuristic Analysis of the Effect of Scale

Notation:

meas@test measured result of a test

calc@test S-Relap5 calculated result of a test

meas@LOCA measured result of a LOCA

calc@LOCA S-Relap5 calculated result of a LOCA

Of the above four the only one we cannot do is the meas@LOCA, yet it is what we want to estimate since it is considered the "truth".

Let P be a variable of interest such as peak clad temperature.

$\therefore P(\theta)$ where θ = set of independent variables defined by PIRT and for which the sensitivities have been quantified.

So, scaling issues deal with the effect of $\theta_{test} \equiv \theta_0 \rightarrow \theta_{LOCA} \equiv \theta_0 + \Delta \theta$ on $P(\theta)$.

If scaling holds ∞

$$P(\theta_0 + \Delta \theta) - P(\theta_0) \propto \Delta \theta .$$

The question then is what are the conditions on test scaling and code scaling so that we can get an estimate of the "truth" in terms of meas@test, calc@test, and calc@LOCA.

Consider the following relationships:

Test Scaling:

$$P^{meas@test}(\theta_0) \rightarrow P^{meas@LOCA}(\theta)$$

Under the assumption that the tests are scalable

$$P^{meas@LOCA}(\theta) \equiv P^{meas@test}(\theta_0) + \partial P / \partial \theta |_{meas@test} \Delta \theta$$

$$\square \quad P^{meas@LOCA}(\theta) / P^{meas@test}(\theta_0) \equiv \{ 1 + 1/P \partial P / \partial \theta |_{meas@test} \Delta \theta \}$$

Similarly for

Code Scaling:

$$P^{calc@LOCA}(\theta) / P^{calc@test}(\theta_0) \equiv \{ 1 + 1/P \partial P / \partial \theta |_{calc@test} \Delta \theta \}$$

What we want to estimate is the "true" value of $P(\theta)$ at LOCA conditions, i.e., we want to compute $P^{meas@LOCA}(\theta)$ at some level of confidence.

From the above expressions we form

$$\frac{P^{meas@LOCA}(\theta) / P^{meas@test}(\theta_0)}{P^{calc@LOCA}(\theta) / P^{calc@test}(\theta_0)} \equiv \frac{\{ 1 + 1/P \partial P / \partial \theta |_{meas@test} \Delta \theta \}}{\{ 1 + 1/P \partial P / \partial \theta |_{calc@test} \Delta \theta \}}$$

Rearranging terms we obtain

$$P^{meas@LOCA} \cong P^{calc@LOCA} * (P^{meas@test}/P^{calc@test}) * \{1 + 1/P \partial P/\partial \theta_{meas@test} \Delta \theta\} \{1 + 1/P \partial P/\partial \theta_{calc@test} \Delta \theta\}^{-1}$$

for $|1/P \partial P/\partial \theta_{calc@test} \Delta \theta| < 1$ we can write

$$P^{meas@LOCA} \cong P^{calc@LOCA} * (P^{meas@test}/P^{calc@test}) * SF$$

where we define a scaling factor (SF) as

$$SF \cong \left(\overbrace{1 + 1/P \partial P/\partial \theta_{meas@test} \Delta \theta}^{\text{test scaling}} - \overbrace{1/P \partial P/\partial \theta_{calc@test} \Delta \theta}^{\text{code scaling}} \right)$$

So, the estimate of the "true" RLBLOCA value of some parameter P has the following components:

- a) $P^{calc@LOCA}$ - the S-Relap5 computed parameter for the LOCA.
- b) $P^{meas@test}/P^{calc@test}$ - the bias estimated by comparing computed and measured values of the parameter from tests. This is the sole source of variation that contributes to the computation of the confidence level in the estimate of $P^{meas@LOCA}(\theta)$.
- c) SF is a factor that accounts for scaling effects.

In my view your analysis implies that $SF = 1.0$. The above discussion implies that for this to be true we must fulfill the following conditions:

- a) $|1/P \partial P/\partial \theta_{calc@test} \Delta \theta| \ll 1$
- b) $1/P \partial P/\partial \theta_{meas@test} \Delta \theta \cong 1/P \partial P/\partial \theta_{calc@test} \Delta \theta$

The first implies that the sensitivities of the computed results of the tests to changes in the independent variables are small. The second that the sensitivity of the measured results for the tests are comparable in size to those computed.

How do your conclusions with regard to test scaling for blowdown, refill and reflood fit into the above scheme?

Similarly, how do your conclusions with regard to code scaling fit into the above scheme?

Response 88: Scaling discussions were separated into test scaling and code scaling in the documentation. The purpose of the discussion with regard to tests was to show that the tests, as they were scaled (or not in the case of the UPTF tests), could predict the LBLOCA phenomena equally well and that there were no discernible effects attributable to the scale of the test facility. For the blowdown phase, it was shown that the peak temperature during the

blowdown was independent of test scale for tests from about 1/6 full scale to tests that were 1/17,000 of full scale. For reflood, a comparison to a similar range of scaled facilities was used to show the independence of the heat-up during reflood (beginning with the liquid at the bottom of the core). For the refill period, full-scale tests were used.

The test scaling condition can be expressed mathematically as

$$P_{Test}(\vec{\theta}') = P_{LOCA}(\vec{\theta})$$

where the $\vec{\theta}$ denotes the parameters which enter into the calculation of the parameter of interest, P . The arrow above is used to indicate a vector. These parameters include those listed in the PIRT table as well as some dimensions. The prime on the vector indicates that it is the vector for the scaled test.

$$\vec{\theta}' \equiv S \cdot \vec{\theta}$$

where S is a matrix which scales the parameter vector. The scaling matrix is by nature a fairly sparse matrix, as the scaling effects need to be applied only to the extensive parameters. The scaling equation then asserts that the measured value of P in the scaled system must be the same as that in the full-scale system for a comparable range of conditions. Only tests for which the scaling condition applies are useful in establishing the test database for the LBLOCA.

The formulation presented in the reviewer's question assumes that the conditions of the tests differ from those in the LBLOCA and that these differences exclude extensive properties that were scaled for the test. This is, in all probability, true. Although scaling of extensive parameters may have been intended, the use of a first-order estimate seems to argue against such an interpretation. Many of the tests were designed to span the conditions that would be expected to occur in a LBLOCA, thereby establishing a basis for analyzing the LBLOCA, provided the analysis tool also scales. For tests consisting of a small number of runs, or even a single run, the conditions were selected to be most representative of the LBLOCA.

Code scaling is important because the code predictions are validated based on small-scale tests and then applied to the full-scale LBLOCA. Scaling discussions in the documentation for S-RELAP5 addressed the extent to which the code predictions might be scale dependent. Several tests with different scaling were evaluated to demonstrate that the code predictions were insensitive to the scale of these tests. In addition, various elements of the code were examined for possible scale effects.

The code scaling relationship can be expressed mathematically as

$$P_{Calc}(\vec{\theta}) = P_{Calc}(\vec{\theta}')$$

where the subscript "Calc" denotes the S-RELAP5 value. This relationship says that the code calculations for scaled test conditions will be the same as the predictions for the full-scale LBLOCA. In this case, the scaled test has to satisfy the test scaling condition.

S-RELAP5 is compared to the test data and biases are determined. Denoting the matrix of biases by M , this process can be summarized by the expression

$$\bar{P}_{Calc}(M \cdot \bar{\theta}') = \bar{P}_{Test}(\bar{\theta}')$$

where the subscript "Calc" denotes the S-RELAP5 value and the bar indicates the mean. Note that the biases have resulted in the code predictions matching the test data in an average sense. Taking into account the uncertainties, the expression can be written as

$$P_{Calc}(\bar{\psi}') = P_{Test}(\bar{\theta}')$$

where

$$\bar{\psi}' \equiv (M + \varepsilon) \cdot \bar{\theta}'$$

and ε is a matrix of random variables representing the uncertainties in the biases. This relationship applies in a statistical sense. That is to say, when the S-RELAP5 calculations are performed using the statistically-varying parameter vector, the probability distribution of the calculated P match those of the test data.

Now, if the code (and the model) with the biases can be scaled from the test conditions to the full-scale, the following relationship can be written

$$P_{LOCA}(\bar{\theta}) = P_{Calc}(\bar{\mathcal{G}})$$

where

$$\bar{\mathcal{G}} \equiv (M + \varepsilon) \cdot \bar{\theta}$$

and the relationship is again understood to apply in a statistical sense.

While the above cannot be expressed as a simple ratio, the points regarding conditions to be met remain valid. The first condition the reviewer places requires the fractional change of the calculated P at LBLOCA conditions from that at test conditions to be small. In addition to requiring a well-behaved calculational tool, it also places a requirement on the sufficiency of the data. The requirement is that the test cases be sufficiently close to the conditions found in the LBLOCA that the fractional variation in the calculated P from the measured P be small. This requirement is met by the use of multiple prototypic tests to evaluate the LBLOCA.

The second condition requires that the predictive model (S-RELAP5 and methodology) display the same dependence on the independent variables as does the test data. This is verified by comparison to a large number of tests, both separate effects and integral, at a large range of scales.

Question 89: 5.1.1 Determining Important Process Parameters

You state "In contrast, treating these process parameters statistically accounts for higher order behavior by including all possible combinations in the sample space."

Question 89a: *What exactly are you referring to by higher order behavior? Give an illustrative example.*

Response 89a: In a typical deterministic assessment, the sensitivity of one parameter is studied at one condition. The choice is often comparable to retaining the linear term in a Taylor series. At points away from that condition, the quadratic term, cubic term, etc. start to have an impact. In addition, the cross-terms with other variables may arise. Then the sensitivity in the variable becomes much different. Consider decay heat sensitivity. At very low PCTs it has one value. Now let the metal-water reaction begin. The sensitivity is suddenly much larger. The higher order behavior in this case refers to all those things in the LBLOCA that make the linearized sensitivity result, taken at one condition, not fully applicable.

Question 89b: *To get "all possible combinations in the sample space" would require n^9 (from Table 5.1) uniformly distributed sample points, where n is some appropriate number of observations for each variable. Is this what you have in mind? This gets big very quickly!*

Response 89b: True. If a census is performed on these combinations the numbers become unmanageable very quickly. In fact, the number of variables in Table 5.1 is much larger than 9. There are 9 categories, but at least 21 variables. So the number is even larger than you have suggested. In the statistical method used for LBLOCA, the presence of a continuum of levels is implicit. By randomly sampling them, the potential for any of the possible combinations of input variables exists. Since the sample size is limited, not all are used to get the final result. However, no combinations are excluded.

Question 90: *5.1.2 Role of Sensitivity Studies*

"Parameters can be demonstrated to be insignificant by sensitivity studies and/or by their relationship to low-ranked PIRT parameters."

Question 90a: *What exactly is meant by sensitivity studies in this context? That is, are these S-Relap5 calculations of a full scale RLBLOCA wherein input parameters are varied? Give an example.*

Response 90a: A large collection (>50) of uncertain parameters (some from the PIRT and some from Plant operation) were identified early on. Estimates of the range of uncertainty that should be associated with each of these were made. A 3-loop Westinghouse Plant model was then run first nominal, then with each of the uncertain parameters adjusted to its maximum (one run per parameter) and then with each adjusted to its minimum. The variation of the PCT for each of these cases was used as a basis for setting the sensitivity. This same process was repeated at an overpower condition to get the PCTs closer to 2200°F to see if the sensitivities were that much different and finally again with a 4-loop Westinghouse plant.

Question 90b: *Have you shown that the results of a S-Relap5 calculation for sensitivity at full scale is valid?*

Response 90b: This question raises the issue of the scalability of sensitivities again. The scalability of the tests used and the scalability of the models within S-RELAP5 were evaluated. In addition, the full-scale model was checked to assure that it conforms to the methodology. The runs were checked and all appear to be acceptable. A series of tests for code stability and repeatability were made to confirm that the variations in the code from numerics and

convergence are small compared to the significant contributors to the PCT changes. These things together support the validity of the S-RELAP5 sensitivities for a full-scale LBLOCA.

Question 91: 5.1.3 Quantifying Statistical Quantities

Why are there no measurement uncertainties associated with the parameters - accumulator level through core flow in Table 5.4?

Response 91: [

]

Question 92: *How are the operational and measurement uncertainties combined to give the distribution for the parameters in Table 5.4?*

Response 92: [

]

Question 93: 5.2 Performance of NPP Sensitivity Calculations

5.2.1 Statistical Approach

Your statement "Non-parametric statistical techniques are useful in situations where acceptance or rejection is based on meeting a tolerance limit and where you do not need the probability distribution itself." is misleading. The analytic form of the probability distribution function need not be known, but the function must be continuous. In the current context, the distribution function is the S-Relap5 code. What evidence do you give that S-Relap5 computed PCT and cladding oxidation are continuous in the independent random variables for RLBLOCA analysis conditions?

Response 93: There are two pieces of evidence which suggest that the S-RELAP5 computed PCT and oxidation are continuous in the independent random variables for RLBLOCA conditions. The first is that the underlying correlations used in the code are continuous. Framatome ANP spent considerable effort to assure that the intersection of different correlations for the same parameter was smooth and continuous. The second piece of evidence is that the PCT as a function of time for each of the 59 cases is continuous. The independent variables experience large changes in value as a function of time during each case. If significant discontinuities existed they would be expected to be visible during at least some of the cases.

Question 94: *Define your use of the term "outlier" in the current context of your application, i.e. given 59 observations of PCT, what makes you call the 59th term in the order statistic and outlier? What statistical test do you apply and what make you think it is appropriate, i.e. not due to some deterministic quirk in the computation? Please formulate your test for an outlier in terms of a statistical hypothesis test.*

Response 94: The use of the term outlier in Section 5.2.1 is misleading since the term outlier has a specific meaning in the statistical sense which is not meant in this section. Framatome ANP proposes to delete the paragraph where the term outlier is used.

The following paragraphs will be inserted in place of the current paragraph on page 5-11 which contains the term outlier. A replacement paragraph is needed because the actions described in the paragraph are still necessary.

It is possible that the result of the 95/95 estimate from the 59 cases will be a PCT that exceeds the 2200 F limit. There are two actions that can be taken in this situation. First a change in the reactor conditions that are being evaluated can be made in an effort to create a set of conditions where the 2200 F limit will not be violated. The changed reactor conditions could consist of a revised total peaking factor limit, or a revised accumulator level, or a revised ECCS injection rates.

A second approach would be to run an additional 34 cases generated with the same seed as the previous 59 cases to obtain a total of 93 cases. For 93 cases the 95/95 estimate is the second highest value rather than the highest value (as it is for 59 cases). Experience with order statistics shows that the 95/95 estimate from 59 cases is, in general, more conservative than the 95/95 estimate from 93 cases. This second approach is only useful for those cases where the 95/95 estimate of the PCT from 59 cases is significantly higher than the PCTs for all the other 58 cases. . Framatome ANP does not plan to use more than 93 cases since we believe that the potential for a conservative answer from 93 cases is too low to warrant the expense of additional cases.

Question 95: *5.4 Determination of Total Uncertainty*

The final results for the 4-loop sample problem are summarized as:

- *The 95/95 calculated PCT was 1635 F*
- *The 95/95 calculated maximum nodal oxidation was 1.1%*
- *The 95/95 calculated maximum total oxidation was 0.02%*

Question 95a: *Are these joint estimates based on the same n = 59 S-Relap5 runs?*

Response 95a: The estimates for PCT, maximum nodal oxidation and maximum total oxidation are not joint probability estimates.

The following statement is made in Regulatory Guide 1.157 with respect to the estimates to be made for the three criteria together.

"The revised paragraph 50.46(a) (1) (i) requires that it be shown with a high probability that none of the criteria of paragraph 50.46(b) will be exceeded, and is not limited to the peak cladding temperature criterion. However, since the other criteria are strongly dependent on peak cladding temperature, explicit consideration of the probability of exceeding the other criteria may not be required if it can be demonstrated that meeting the temperature criterion at the 95% probability level ensures with an equal or greater probability that the other criteria will not be exceeded."

Framatome ANP will modify the submitted methodology to calculate the 95/95 PCT value and report the other two parameters for this case consistent with the Regulatory Guide. Demonstration that the PCT is met with 95% probability and 95% confidence assures that the two criteria related to oxidation will be met with an equal or greater probability. This is because of the strong correlation between cladding temperature and oxidation and because the margin to the criteria limits is much greater for the oxidation criteria than for the temperature criteria (see Table 5.9).

Section 5.2 of EMF-2103 will be revised to reflect this change in statistical approach. The change pages for Section 5 are presented in Appendix C. Changes to the text will be made on the original pages 5-11, 5-15, 5-16, 5-17, and 5-18. Tables 5.10, 5.11, and 5.12 will be deleted. Figures 5.4 and 5.5 will be deleted. Appendix D will be revised in a similar manner when the approved document is issued.

Question 95b: *If yes, please explain why. The 95/95 for the joint estimation of three dependent variables requires far more than $n = 59$.*

Response 95b: That is generally true, but these are not joint estimates.

Question 95c: *Physically PCT and oxidation rates should be correlated. Do you account for that and if so how?*

Response 95c: S-RELAP5 calculates oxidation rate using the Cathcart-Pawel equation which correlates oxidation rate as a function of absolute temperature. Therefore, the oxidation rate is functionally dependent on the cladding temperature in S-RELAP5. As a result, PCT and oxidation are highly correlated.

Question 96: *Stored energy in the fuel is treated, however pin pressure is not. Please describe the methods used to assess the potential for blowdown ruptures and how fuel rod gap pressures are calculated and treated statistically.*

Response 96: Fuel pin pressure is treated by the methodology; initial fuel rod pressure is calculated with RODEX3A and transient fuel rod pressure is calculated with S-RELAP5 using the same fuel models as RODEX3A. A principal reason for incorporation of the RODEX3A fuel models into S-RELAP5 was to provide a fuel rod pressure calculation consistent with the initial

conditions from the approved RODEX3A model. S-RELAP5 and RODEX3A account for pin pressure variations as a result of changes in pellet and clad dimensions and gas composition.

Pin pressure can influence two LOCA phenomena given in the PIRT in Table 3.4 in the methodology document: stored energy and gap conductance. Table 4.18 briefly lists how each phenomena is treated. [

]

Fuel rupture is not treated in this methodology as is discussed in Appendix B.2. Rupture of fuel rods, when predicted, does not occur during blowdown, because the relatively high system pressure reduces the pressure differential across the cladding during this phase of a LOCA. If calculated, fuel rod rupture typically occurs during refill and possibly could occur late in the refill phase of a LOCA. Framatome ANP showed that fuel rupture, when calculated, has the beneficial effect of slightly reducing PCT. Since the general influence of fuel swelling and rupture was relatively small and beneficial, we chose to be conservative and ignore this effect and to focus on other methodology development areas. (Also see response to Questions 28a and 131)

Question 97: *Please explain how the uncertainty in the gap gas conductance is accounted for. Please explain how variations due to fuel relocation are treated and included in the uncertainty in the stored energy of the fuel.*

Response 97: [

]

Question 98: *What is the initial oxide layer thickness assumed on the inside and out side of the rod. Please explain how this is treated and justify the initial oxide layer thicknesses.*

Response 98: The initial oxide layer thicknesses on the outside and inside of the cladding are calculated as a function of burnup for each axial node in the RODEX3A calculation. The axially dependent oxide layers are then passed to the S-RELAP5 calculation and are used in the calculation of cladding thermal conductivity which affects the initial stored energy. [

]

Question 99: *On page 4-94, the 90% confidence limit was used to evaluate the constant and exponential terms in the oxidation model. As described in Regulatory Guide 1.157, please use the 95 percentile confidence limits to evaluate these terms. Also, was the uncertainty on the predicted mean of the data in the Cathcart-Pawel cited reference verified.*

Response 99: The 95% limit was obtained by noting that for a normal distribution, the two-sided 90% limits correspond to the 95% upper limit and the 95% lower limit. The statistics on the Cathcart-Pawel model were not reevaluated. This reference is heavily cited and has been reviewed by the NRC as documented in NUREG-1230, Compendium of ECCS Research for Realistic LOCA Analysis.

Question 100: *Cold leg condensation, only, is discussed on page 4-99. Please explain how downcomer condensation was ranged and applied in the methodology.*

Response 100: [

]

Question 101: *Downcomer entrainment was not discussed in the statistically treated section. Please explain how downcomer entrainment was ranged.*

Response 101: The code calculation of downcomer entrainment is addressed in the methodology by demonstrating that the combination of code models and plant nodalization used in the methodology results in a conservative prediction of the lower plenum fill rate. This conservatism was demonstrated by comparison with the UPTF Tests 6 and 7 and is discussed in Section 4.3.3.1.10 of EMF-2103.

Question 102: *The refill heatup period heat transfer multipliers were also not discussed. Please show the S-RELAP5 code predictions to data during refill and show the heat transfer multipliers applicable to refill.*

Response 102: As part of determining the film boiling heat transfer multipliers, it was necessary to consider the application in which those multipliers are used and compare this range to the available data. The summary results of this evaluation were presented in Table 5.1 of EMF-2102, which identifies the range of key parameters needed for the RLBLOCA application, as compared to the range that is available from the data used to develop the film boiling heat transfer multipliers. The information in this table were derived independent of the transient phase, that is, they represent conditions from blowdown, heatup, and reflood. This was important because in S-RELAP5, the core film boiling heat transfer models are applied any time film boiling is indicated – the same models are used for blowdown, heatup, and reflood. Figures 1 and 3 of RAI Response #2 show the clad rod temperature response during blowdown, heat-up, and reflood at two different PCT locations. The void fractions in the heatup region are well within the range supported by the film boiling multipliers. The pressures observed during the heat-up are also supported. On this basis, the heat transfer multipliers that support heat-up are FILMBL=1.00 and FRHTC=1.75.

The S-RELAP5 predictions to data during refill are shown in the following figure. []



Question 103: *Please explain the "Comparison with Adjusted Accumulator" in Fig. 4.152.*

Response 103: In the original data obtained by Framatome, the measured accumulator volumetric flow rate was provided. In the initial performance of the analysis, the analyst missed the fact that when the accumulator emptied the flow switched from liquid to nitrogen. The title on the plot simply reflected the fact that the final analysis had accounted for this switch from liquid to nitrogen flow.

Question 104: *LOFT L2-3 predictions capture the second peak due to the lack of quench during blowdown. If quench occurs, how well does S-RELAP predict the second peak? Do the plant calculations always show a failure to quench during blowdown? If not what is the effect on the reflood PCT?*

Response 104: Since the code under-predicts heat transfer under low void conditions, a second heat-up should over-predict the data. Of the 3-loop and 4-loop plants, the 4-loop plant is most likely to experience quenching immediately after the blowdown peak. The submitted 4-loop plant calculation does not show that behavior.

Question 105: *Explain why the methodology does not contain an uncertainty assessment regarding peak local oxidation. At the higher PLHGRs and with downcomer boiling, what is the core wide oxidation.*

Response 105: In the last paragraph of Section 5.4 (EMF-2103) a statement is provided specifying an uncertainty assessment of PCT, peak local oxidation (a.k.a. maximum nodal oxidation), and core wide oxidation. This is provided in terms of the 95/95 and 50/50 results. In general PCT results are emphasized since the temperature limit is much closer to calculated PCT results likely from an LBLOCA analysis and since the oxidation variables are primarily dependent on clad temperature.

Other conditions being equal, at higher PLHGRs and at low containment pressures in which the effects of downcomer boiling would be expected to be the strongest, clad temperatures would likely remain high for a longer period of time. To ensure an accurate accounting of oxidation variables, a calculation is not terminated until the clad temperature at the peak power node drops below 1200°F and the transient time is greater than 300 s (guillotine breaks) or 400 s (split breaks). At temperatures below 1200°F, oxidation rates are not significant enough to appreciably increase the total oxidation. Nonetheless, most cases run out to total core quench.

Question 106: *What is the basis of the moderator-density feedback curve employed in the analysis? Is the most positive MTC allowed by the Tech. Specs. used? Please explain and show the reactivity versus density curve used in the demonstration analysis. What doppler feedback curve is used? What is the uncertainty in these curves applied to the analysis?*

Response 106: [

]

Question 107: *In Table 5.7 on page 5-23 of EMF-2103, how was the lower limit on T inlet determined? Will the analysis be applied to plants during an end of cycle coastdown? If so, what is the sensitivity of the methodology to T inlet and how would the evaluation be performed?*

Response 107: Core inlet temperature is a plant parameter which is sampled over the range of operation of the plant. It is expected that the utility customer will supply this information and supporting data to Framatome. Sensitivity studies on the effect of perturbations of this parameter on PCT showed that PCT was relatively insensitive to core inlet temperature over the normal operational range. For the 3- and 4-loop sample problems, no account has been made for end-of-cycle coastdown; however, because of the power coastdown, conditions typical of end-of-cycle coastdown are not expected to challenge LOCA acceptance criteria as much as earlier periods in the cycle.

For plants that apply an end of cycle coastdown, a number of parameter ranges may change during this period. This RLBLOCA methodology already addresses time-in-cycle variations from a neutronics and burnup perspective. Hence, the end of cycle coastdown will be addressed through the sampling of time-in-cycle dependencies and programming the model changes that correspond to that coastdown period.

Question 108: *In Fig. 5.2 on page 5-29 of EMF-2103, which peak temperatures are due to first peaks and which are due to reflood peaks? The peaks corresponding to times beyond 100 seconds are very low. These appear to be reflood peaks; please explain why the reflood peaks are so low when linear heat rates are based on peaking factors in the range 2.4 to 2.6? Why do the guillotine breaks appear to be all first peak limited?*

Response 108: This sample problem is representative of a 4-loop PWR. The PCT signature predicted by S-RELAP5 for the 4-loop problem will typically show a blowdown peak within the first 10-15 s and then a single reflood peak between 30-60 s. With emergency core cooling coming from 3 intact loops, the two-peak characteristic is not a surprising result. For the smaller split breaks the emergency core cooling is more than adequate to suppress clad temperatures; hence, those cases showing a late reflood peak (> 100s) will typically be those smaller split breaks. A 3-loop PWR sample problem has been supplied as Appendix D of EMF-2103 Revision 0. The PCT signature from the 3-loop problem does show cases having either a blowdown peak, an early reflood peak, or a late reflood peak.

Question 109: *Fig. 5.3 show break areas of 1.0 ft² and less. What is the effect on the PCT distribution if breaks 1.0 ft² and smaller are thrown out? The upper limit on the break size is about 4.0 ft². What are the break multipliers for the largest sizes in Fig. 5.3? How are the multipliers applied to each side of the break? Please explain.*

Response 109: Following the statistical discussion provided in Section 5.2.1, if, for example, the 10 cases with break sizes less than 1.0 ft² were removed, the limiting calculation would still represent about a 94/95 coverage/confidence (i.e., $(0.94)^{49}=0.05$). Performing the 59 cases excluding breaks smaller than 1.0 ft² would have some likelihood (10/59 = 17%) of exceeding the limiting PCT calculation; however, the probability that the resulting PCT would be significantly greater than the next highest PCT would be small.

[

]

Question 110: *What does the scatter plot for PCT versus reflood rate look like?*

Response 110: The reflood rate varies over a very wide range during the LBLOCA and one would have to define some sort of weighted average of the time-dependent reflood rate values to create the requested plot. Reflood rate is not a parameter that Framatome ANP considers in the LBLOCA, other than to assure that the range of reflood rates experienced during a LBLOCA are covered in the validation database. Since the dependence on axial power shape, film boiling heat transfer, and break size are so strong, it is likely that if the requested plot were created, it would look like a typical random scatter plot. Such a plot would not have much value from an analytical point of view.

Question 111: *Table 5.7 identifies the failure of 1 LPSI and 1HPSI. Please show the PCTs for a diesel failure, an LPSI failure, and no failure on the same plot.*

Response 111: [

]

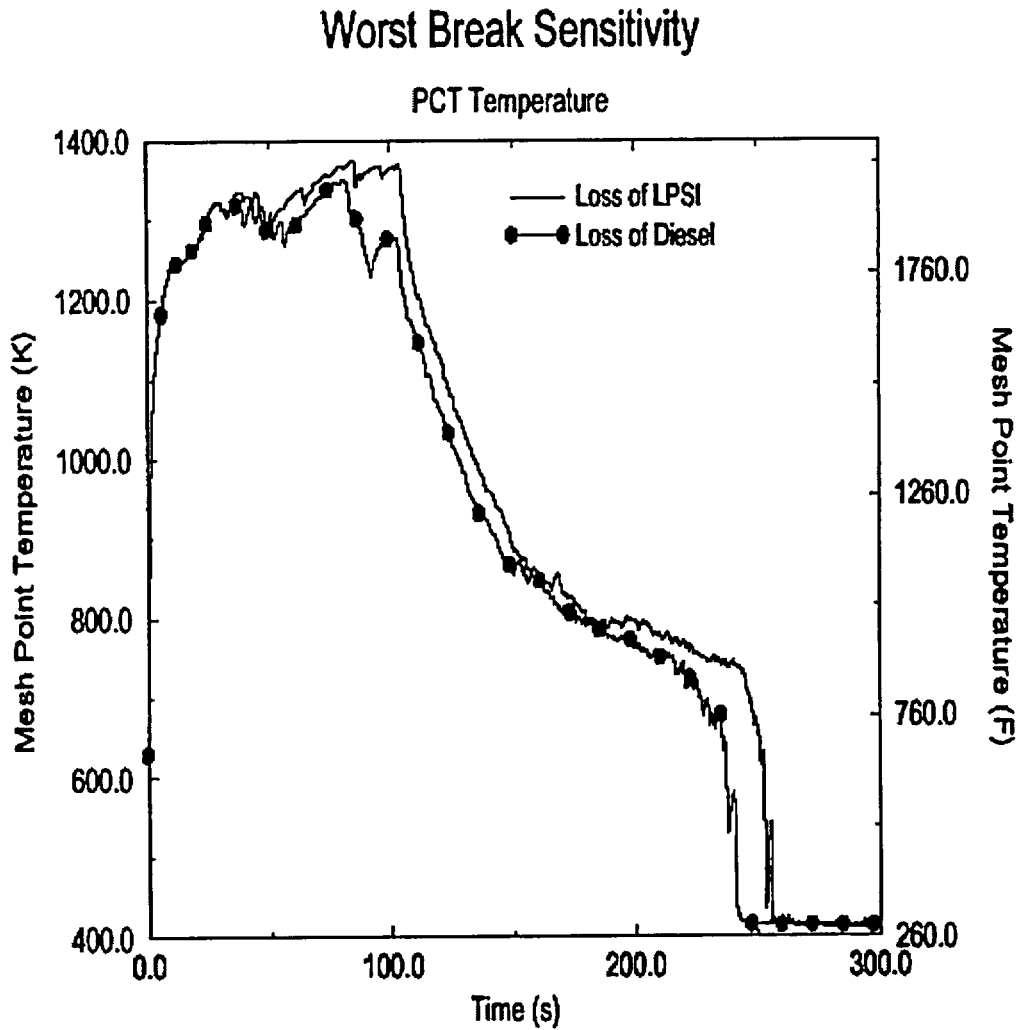


Figure 11.1 Clad Temperature Response from Single-Failure Study

As a followup to this study, another study has been performed analyzing a suite of single-failure assumptions including the no failure assumption. This study has been applied to a low containment pressure plant simulation. The specific calculations are summarized in the following table:

--	--

[



Figure 111.2 Clad Temperature Response from Single-Failure Study



Figure 111.3 Containment Pressure Response from Single-Failure Study



Figure 111.4 Liquid Level Response from No Failure Simulation

Question 112: *In Table 5.7, why is SG plugging limited to 10% since the average for operating plants is 15%? How is the plugging distributed among the SG? How are asymmetries in plugging handled?*

Response 112: In the sample problems, steam generator tube plugging has been set to 10%. This value is arbitrary for this analysis. For an actual analysis, this information would be provided from the utility customer and likely be adjusted to meet the demands of plant operation. Sensitivity studies on tube plugging show very little impact on PCTs; however, the increased flow resistances do contribute to somewhat lower reflood rates and, hence, core cooling precedes at a rate slower than with steam generators with no plugging. To support subsequent fuel cycles, utility customers usually request that steam generator tube plugging be set higher than current cycle conditions. If steady-state loop flows are significantly impacted, asymmetry in steam generator tube plugging must be considered. Since each steam generator is modeled separately, asymmetric plugging levels can be incorporated by adjusting geometries and flow losses as appropriate in each steam generator.

Question 113: *Table 5.7 lists the hot assembly to be anywhere in the core? Please show the core flow and PCT for the hot assembly placed in the most limiting position which minimizes blowdown cooling.*

Response 113: The position of the hot assembly in the core refers to its placement relative to other assemblies in the core and structure in the upper plenum. For LOCA, the influence of the other assemblies is driven by the radial power distribution in the core. The radial core nodalization is always as that shown in Figure 4.7 of the methodology document. [

]

Question 114: *Minimum EC boron of 2925 is used in the analysis. What is the minimum time to boron precipitation for this boron concentration? Show that the switch to simultaneous injection occurs before precipitation for the limiting large break and location.*

Response 114: See the response to Question 32.

Question 115: *Please explain why the PCT is not skewed toward the higher values as power is increased in Fig. 5.6 of EMF-2103 and F_q is increased in Fig. 5.7?*

Response 115: In most of the PCT scatter plots in Figures 5.2-5.16, an obvious trend is difficult to discern. These figures are presenting the PCT results from the same set of 59 calculations through many different "filters." Because so many parameters are being varied, only the few most dominant parameters will show a correlation with PCT. [

]

Question 116: *How is the ASI chosen in the analysis? Are power distributions with power skewed toward the top most likely and how does the ASI chosen reflect the most likely distribution?*

Response 116: [

]

Question 117: *Please explain why the trend in PCT is not increasing with increasing inner ring and cold ring power? Are these PCTs determined with the hot assembly located in the position which minimizes core flow and cooling during blowdown? Which PCTs are first peaks?*

Question 118: *What do the PCT scatter plots look like if they are separated into first peaks and second peaks?*

Response 117 and 118: [

]

Figure 5.2, which shows the PCT vs. Time-of-PCT, can be used to differentiate first versus second peaks. There are about 10 cases showing a blowdown PCT in Figure 5.2. These all occur before 20 s. The break area has such a strong influence on the time of PCT (blowdown PCT and first or second reflood peak) that it masks any other potential trends.

Question 119: *Why does the PCT turn around so quickly in Fig. 5.18? What is the reflood rate versus time for this break? Please explain why the quench occurs so early since downcomer*

boiling should initiate following discharge of the SITs.

Response 119: The PCT turns around quickly because there is water in the core. The 4-loop PWR LBLOCA benefits from the early blowdown cooling (see Response to Question 120), which removes considerable stored energy from the rods at lower elevations. Consequently, the core is "easier" to quench during the reflood phase. Figure 119.1 shows the core average reflood rate. The ECC water from the intact loop accumulators reaches the cold legs at about 14 seconds. At about 32 seconds, the water reaches the bottom of the core. During the rest of the accumulator injection period (up to about 60 seconds), the ECC water injection rate to the core (reflood rate) is about 12 cm/s (4.7 in/sec). The reflood rate drops to about 2.5 cm/s (1 in/s) after the accumulators are empty. The blowdown cooling and the flow of the accumulator ECC water into the core are responsible for the early quench of the lower part of the core. Figure 119.2 shows the heat transfer rate from the downcomer walls and other structures to the fluid in the downcomer. It is seen that the heat transfer rate to fluid is over 50 MW during the accumulator injection period. However, boiling is limited to near the surface region since the ECC water and, therefore, the bulk of the fluid is highly subcooled as depicted in Figure 119.3, which shows the liquid subcooling at the axial level (Level 3) below the ECC injection level (Level 2).

Note: A short period of negative reflood rate occurs around 270 s. As a consequence of core quench at around 220 s, there is a period of increased vapor flow. As this period of increased vapor dissipates, there is significant liquid fall back to the core from the upper plenum. Using the simple reflood rate approximation applied to generate Figure 119.1, this appears as a period of negative reflood rate.



Figure 119.1 Average ECC Water Injection Rate into the Core



Figure 119.2 Heat Transfer Rate to Downcomer Fluid from Walls and Structures



Figure 119.3 Liquid Subcooling in Downcomer at Axial Level 3 from the Top (One level Below the ECC Entrance to Downcomer)

Question 120: *What is the cause of the spike in flow at about 7.5 seconds in Fig. 5.20? What is the PCT if this flow spike is eliminated?*

Response 120: Figure 120.1 shows the sum of mass flow rates from the four cold legs to the downcomer and the mass flow rate from the lower plenum to the core. The flow from the broken cold leg to the downcomer is negative (out of the downcomer). At the beginning of the transient, the magnitude of the broken loop flow is much larger than the sum of the three intact cold leg

flows and the net flow to the downcomer is negative. Thus, liquid flows from the downcomer and three intact loops to the break. To supply the additional break flow, liquid also flows downward from the core to the lower plenum and up the downcomer to the break. This produces the early core flow reversal. As the system pressure rapidly decreases, the magnitude of the critical flow at the break decreases substantially due to the change in upstream conditions as depicted in Figure 5.19 of EMF-2103(P). During this time, the flow from the three intact cold legs does not change much due to the flow inertia and the short available time for pump coastdown. Consequently after the early core flow reversal, there is a short time period during which the net flow to the downcomer and lower plenum regions is positive. Furthermore, the intact cold legs, downcomer, and lower plenum are still full of liquid. This forces an upward flow through the core. This is a well-known characteristic of the 4-loop plant LBLOCA. For this particular calculation, the positive flow period is between 3.3 seconds and 5.6 seconds. The positive flow reaches the core at about 5 seconds. This positive core flow is real and can produce core quench during the blowdown period, as experimentally observed in the LOFT L2-3 and L2-6 tests. However, S-RELAP5 calculates enhanced blowdown cooling but no quenching due to this effect. The positive flow into the core during this blowdown period is a real physical phenomenon; it cannot be eliminated.



Figure 120.1 Sum of Mass Flow Rates from Cold Legs to Downcomer and Mass Flow Rate from Lower Plenum to Core

Question 121: *What is the cause of the downcomer level increase just after 50 seconds in Fig. 5.25? What causes the drop in level at 225 seconds? Please show a plot of the downcomer void fractions versus time. Also show a plot of the downcomer temperatures for these locations versus time compared to the saturation temperature.*

Response 121: Continuing accumulation of ECC water in the downcomer is the cause of the downcomer level increase. The quenching of the bottom of the core retards the water flowing into the core and the accumulator water flowing into the downcomer is rather strong; therefore, more water is accumulated in the downcomer. At around 200 seconds, the high power region (middle upper elevations) of the average and hot channels quenches within a few seconds between different axial elevations. The extra steam generated flows through the intact loop cold legs to the downcomer and carries more water from the downcomer out to the break. This causes the downcomer level to drop. Figure 121.1 shows a plot of downcomer void fraction at axial level 3 (the ECC water entering the downcomer at axial level 2). The water subcooling (saturation temperature – liquid temperature) at the same axial level is shown in Figure 119.3.



Figure 121.1 Void Fractions at Third Axial Level from the Top of the Downcomer

Question 122: *Show a plot of the core flow at the PCT location.*

Response 122: Figure 122.1 shows the vapor mass flow rate at the PCT node (9.4 ft) in both axial and radial directions. The flow in the radial direction is much lower than the axial flow and is positive (flowing out of the volume) during the reflood period. The corresponding liquid mass flow rates are shown in Figure 122.2. The axial flow is rather chaotic. The radial flow is positive before the region is quenched. The chaotic axial liquid flow is inherent with the reflood calculation. The large amount of vapor generated in the quenching volume causes a temporary pressure increase in the volume, which in turn throws chunks of the liquid up and down into the neighboring volumes. A portion of the liquid thrown upward falls back down and some gets carried out of the core by the vapor. Figure 122.3 shows that at the upper tie-plate junction above the hot assembly the liquid flow is always upward and there is no liquid falling down from the upper plenum into the hot assembly.



Figure 122.1 Axial and Radial Vapor Mass Flow Rate at the PCT Node (9.4 ft)



Figure 122.2 Axial and Radial Liquid Mass Flow Rate at PCT Node (9.4 ft)



Figure 122.3 Liquid Mass Flow Rate at the Upper Tie Plate Junction Above the Hot Assembly

Question 123: *Please show the heat transfer coefficient and steam temperatures corresponding to Fig. 5.18. Also show the core void fraction versus time for these locations and the droplet size at the hot spot versus time. What is the reflood rate versus time?*

Response 123: Heat transfer coefficient, steam temperature, void fraction and droplet size are shown, respectively, in Figures 123.1 through 123.4. The reflood rate is shown in Figure 119.1 (see Response to Question 119) Note that the droplet diameter is not used after an elevation is quenched.



Figure 123.1 Heat Transfer Coefficient at Four Elevations



Figure 123.2 Steam Temperature at Four Elevations



Figure 123.3 Void Fraction at Four Elevations



Figure 123.4 Droplet Diameter at PCT Node

Question 124: *Why does the PCT show the rapid temperature decrease just after the SITs empty? What are the LPSI and HPSI flowrates after SIT exhaustion?*

Response 124: (See Responses to Questions 119 and 120 for more detail.) The clad temperature decrease is due to the presence of water in the region. The blowdown cooling discussed in Response to Question 120 contributes to a reduction in PCT. The flow of the accumulator ECC water into the core discussed in Response to Question 119 accounts for about a 30 second period of higher reflood rate. As a consequence, the clad temperature is not too high and there is water in the core. The LPSI and HPSI flow rates are shown in Figure 124.1

In addition, the following phenomena are associated with the emptying of the SITs that contribute to higher ECCS flow and a pressure pulse at this time. As the SITs empty, the ECC lines connecting them must also be cleared. When this happens, the effective pressure drop resistance of the lines (portion in liquid flow) decreases faster than the gas expansion driving the injection. This results in an unbalanced force that accelerates the ECC injection rate as the lines clear. When the lines are cleared, a pressure pulse follows due to the nitrogen when it enters the vessel (see response to Question 126). These two phenomena enhance cooling just as the SITs clear.



Figure 124.1 LPSI and HPSI Mass Flow Rates

Question 125: *Why is the lower plenum liquid solid at about 75 seconds? Why is there no boiling in this region? How is wall heat modeled in the lower plenum? Please explain.*

Response 125: Lower plenum walls and internal structures are modeled. Figure 125.1 shows the total heat power released to the lower plenum fluid from these structures. The heating power to fluid is still about 9 MW at 75 seconds and decreases rather slowly. However, the bulk liquid is highly subcooled, as indicated in Figure 125.2; therefore, boiling is limited to the region close to structure surfaces.



**Figure 125.1 Heat Transfer Rate to Lower Plenum Fluid
from Walls and other Structures**



**Figure 125.2 Liquid Subcooling (Saturation Temperature – Liquid Temperature)
in the Lower Plenum**

Question 126: *What is the source of the pressure spike in Fig. 5.28 at 70 seconds? Please explain.*

Response 126: The pressure rise starts at 60 seconds and reaches a maximum value at 63 seconds. The start of the pressure rise coincides with the emptying of the accumulators. The nitrogen in the accumulators begins to flow into the system when the accumulators are nearly empty. The pressure associated with the nitrogen gas is determined by the initial amount of gas present and the volume to which this gas has expanded. As the nitrogen enters the system its pressure is above that of the system. At this time the system pressure is near the containment pressure. Thus, the calculated system pressure at the injection point rises rapidly to the nitrogen pressure, then decreases as the nitrogen gas is dissipated. The flow of nitrogen into the cold legs also reduces the condensation rate and thus increases the pressure. Nitrogen bubbles can also be trapped between liquid regions and cause pressure to increase.

Question 127: *What is the sensitivity of PCT to the expected variation in containment pressure? What is the uncertainty in containment pressure?*

Response 127: [

]

Question 128: *Page A-4 of EMF-2103 states that a discussion of each study is not practical. In order to demonstrate the basis for these studies plots of key parameters are needed along with a discussion of the results. The basis for each sensitivity needs to be explained and the key plots presented with comparisons to the base case to provide the technical justification for the choices for the parameters listed in the sensitivity studies given in Table A.2.*

Response 128: Sections 4.1.1, 4.2, 5.1.2 and Appendix A discuss the role of sensitivity studies in the development of this methodology. Section 4.1.1 provides detail on how most of these sensitivity studies were performed for the purpose of establishing the Assessment Matrix. Section 4.2 refers to the role of sensitivity studies in the nodalization definition. Section 5.1.2 clarifies the use of results from sensitivity studies within the non-parametric statistical methodology. Appendix A provides an overview of how the sensitivity studies were designed.

In non-parametric statistics, sensitivity studies are not used to develop a response surface. The role of sensitivity studies is basically to confirm the importance of the highly ranked PIRT phenomena and to determine which of the plant parameters are important. Those phenomena and parameters demonstrated through the sensitivity studies to actually impact the predicted PCT are those which will be addressed statistically in the methodology. This list of important phenomena and parameters are then used to define the assessment matrix for determining uncertainties and to define which plant parameters will require data to support their statistical treatment. Thus, the importance of the sensitivity studies in non-parametric statistics is significantly less than in the response surface approach.

Overall, at least 10 calculational notebooks were created documenting approximately 400 sensitivity studies. This documentation is about 3000 pages worth of information and includes the calculational detail requested. If this detail is of interest to the NRC it is available for their review at the Framatome ANP offices.

Question 129: *The discussion in Section A.2 refers to core flow stagnation, reduced heat transfer and many other phenomenological behaviors but does not show any plots other than PCT. Figs A.1 through A.4 do not display quench. Please show the quench for these cases. What is the impact on clad oxidation for these cases? Comparison of Fig. A.3 with A.1 show an increase in PCT of 500 F. Given this large change in PCT and the fact that the S-RELAP5 did not capture the effects of nitrogen which was to subsequently increase PCT after the initial decrease, please provide the justification for including this PCT benefit in the methodology. Is Fig. A.2 incorrectly labeled as this plot for the 4-loop plant? Why does the PCT increase substantially beyond that for the 3-loop plant compared to the 4-loop plant when nitrogen*

injection is precluded.

Response 129: Unlike the parametric statistical approach taken in the CSAU sample problem given in NUREG/CR-5249, sensitivity studies are not used in the development of a PCT response surface. This is not required in a non-parametric approach. The primary application of these sensitivity studies was to determine a relative PCT sensitivity to the many LOCA parameters identified in the PIRT (and from plant operation considerations) and to determine which parameters should be treated statistically. This information serves to define the assessment matrix. The figure-of-merit in this process was chosen to be PCT. For this reason, in the sensitivity studies performed, only PCT vs. time information was recorded. Once PCT sensitivity was determined, the calculation could be terminated. Core quench time is not included in the PIRT; hence, it wasn't necessary to run the calculations out to core quench. Clad oxidation is dependent on clad temperatures and thus does not need to be evaluated separately.

Clad oxidation and accumulator nitrogen were not included in many of the sensitivity studies because they can potentially introduce nonlinear PCT sensitivities that might disguise the true sensitivity of the studied parameters. This is discussed in Section 4.1.1. (Note: one set of 72 sensitivity studies included accumulator nitrogen and another ~35 sensitivity studies were done examining PCT fuel rod parameters such as clad oxidation, these are mentioned in Table A.2.)

Nonetheless, both clad oxidation and accumulator nitrogen are applied in this RLBLOCA methodology (i.e., no benefit has been taken). As a method to evaluate PCT sensitivities to serve in the CSAU decision-making process, this action was judged to be appropriate.

Figure A.2 is incorrectly labeled. It should read "PCT independent of elevation for the 3-loop plant at nominal power without accumulator nitrogen effects". This will be corrected in the document. Three of the four sets of sensitivity studies were performed without including accumulator nitrogen. The cases shown in Figure A.3 and A.4 are described in the third and fourth bullets in the first paragraph of Section A.1.

For the cases referred to by Figures A.3 and A.4, a top skewed axial power profile and an increase in both core and decay power were made to force PCT to occur during late reflood. The relatively higher PCT in the 3-loop base case is the result of a number of differences between the 3- and 4-loop problems; however, the biggest player is probably that emergency core cooling is served through only 2 intact loops in a 3-loop PWR vs. 3 intact loops in the 4-loop PWR.

Question 130: *How does low rod pressure produce more conservative PCTs as indicated in Table A.2? Higher rod pressures at higher linear heat rates will eventually cause blowdown ruptures increasing the stored energy at end of blowdown that will increase PCTs. Please explain.*

Response 130: Table A.2 states that the low rod pressure sensitivity study "produces slightly more conservative PCTs – not significant to range, use nominal values." The actual difference in PCT was 17.3°F. This is within the normal code numerical uncertainty given as [] in Appendix C; hence, the conclusion was that this is not a significant difference and that, for this reason, it is unnecessary to range this parameter.

The likelihood of blowdown ruptures is consistent with the condition of higher rod pressure which is characteristic of high burnup fuel rods. Framatome's experience is that such fuel rods are

present for latter cycle fuel, i.e., once- or twice-burned fuel. Sensitivity studies examining clad temperature sensitivity relative to bumup have shown that sampling from first cycle fuel assemblies, will produce clad temperature predictions which will bound the clad temperatures predictions for previously burned fuel. This has been attributed to the lower power densities characteristic for previously burned fuel.

Question 131: *In the rupture sensitivities given in Figs. B.3 and B.4, how was fuel relocation and the subsequent heat generation in the ruptured zone modeled? If this was not taken into account, please justify the omission of fuel relocation effects in the ruptured region. How does blowdown rupture influence the conclusions of the rupture study? What assumptions are made regarding rupture of the surrounding rods in the rupture study. Are touching strains predicted and what conditions are needed for this condition? What is the justification for the blockages calculated that show rupture reduces PCT? What is the PCT sensitivity to percent blockage up to the maximum? What test data was used to justify the less limiting nature of rod rupture and show S-RELAP5 comparisons to the data?*

Response 131: [

]

[

]





[

]

References

131.1 E. H. Karb et al., *KfK In Pile Tests on LWR Fuel Rod Behavior During the Heatup Phase of a LOCA*, KfK 3028, Kernforschungszentrum Karlsruhe GmbH, Karlsruhe.

Question 132: *Please show the heat transfer coefficient vs time for Figs. B.3 and B.4. Also show the temperature of the node just above the ruptured region and its corresponding heat transfer coefficient. Also show the gap conductance vs time for the ruptured and unruptured region just above. Are the drop sizes affected by the ruptured region. What is the void fraction and corresponding drop sizes versus time at the hot spot?*

Response 132: A sensitivity study of the effect of using a swelling and rupture model is presented in Appendix B of EMF-2103(P). In this study, the rod swelled but did not rupture, though this may not be clear from the discussion. The intent of the original calculations was to examine the rod performance issues in a "bounding manner". Applying the method described in Section 5.1.3.2 of the methodology document (EMF-2103(P)), a limiting hot rod was identified from a large set of neutronics calculations designed to analyze the specific reload cycle. This limiting rod is the rod that is expected to have the highest peak LHGR rate. In the study, the highest LHGR calculated using the method from Section 5.1.3.2 was 11.5 kW/ft. After this rod was identified, the LHGR was increased so that the rod-averaged power (i.e., radial peaking factor) was 80% greater than core average (a bounding value for most, if not all, currently operating PWRs). In the sensitivity studies, this raised the peak LHGR to ~12.5-13 kW/ft, which varies depending on bumup. The specific sensitivity studies presented in Section B.2 were designed to examine the effects of the swelling and rupture model in the S-RELAP5 code. This is the NUREG-0630 model most commonly used in LOCA analyses. In both instances, the use of this model provided a benefit in terms of PCT and oxidation criteria. The conclusion from this study is that it is conservative to neglect swelling and rupture in the methodology. The complexity of the swelling and rupture phenomena is such that it was decided to accept this conservatism in the methodology.

In response to this question an additional analysis has been performed applying the swelling and rupture model (based on NUREG-630) to the limiting PCT calculation presented in Appendix D. The purpose of this was to perform a sensitivity study where rupture did occur. The following

figures provide the requested results from the additional sensitivity study. The first figure presents a PCT comparison for a calculation including the swelling and rupture model vs. the base case. As with the calculations given in Section B.2, PCT is reduced relative to the base case. In addition, examination of the oxidation criteria shows that the base case results also bound the swelling and rupture case. The second figure shows the heat transfer coefficient vs. time for the two cases at node 28 which is the rupture node when the swelling and rupture model is enabled (indicated as "Modeled Enabled" on the figures). Also, from the "Model Enabled" calculation, the heat transfer coefficient is shown for the node immediately above the rupture node. The third figure shows the clad temperature traces at these same three nodes. The last figure shows the gap conductance. The drop in gap conductance which begins around 13 s is from the rod swell. Around 18 s the rod ruptures and the gap conductance drops to its eventual minimum value.

The swelling and rupture model does not take credit for the likely liquid deentrainment that would occur as a result of this condition. In addition, the Forslund-Rohsenow dispersed flow film boiling correlation is unmodified for this condition. The deentrainment phenomenon is expected to be a PCT benefit and by not considering its effects in S-RELAP5, the analyses possess this conservatism. A discussion of void fraction and droplet size at the hot spot is presented in the response to Question 123.

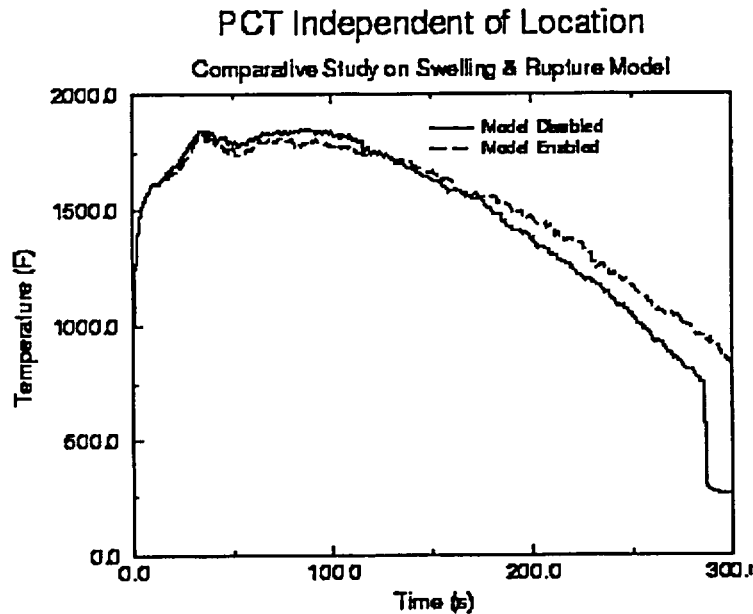


Figure 132.1 Swelling and Rupture Model: PCT Independent of Location



Figure 132.2 Swelling and Rupture Model: Heat Transfer Coefficient



Figure 132.3 Swelling and Rupture Model: Clad Temperatures Near Rupture Node



Figure 132.4 Swelling and Rupture Model: Gap Conductance

Question 133: *Fig. B.13 shows an increasing PCT at the end of the plot. Please show the transient until quench.*

Response 133: The purpose of the sensitivity study presented in Figure B.13 was to assess the impact of pump two-phase degradation model by replacing the best-estimate EPRI model with the Semiscale model (with greater degradation). Following the reasoning used to develop the PIRT ranking for this parameter, the period of interest is blowdown. The phenomenological expectation was that with increased pump degradation, the pumps influence on blowdown cooling would be minimized and that this should be observable in the first 20-50 s; hence, this figure was made to highlight this period of interest.

As mentioned in RAI response #129, the objective of the sensitivity studies was to determine PCT sensitivity to perturbations in a set of PIRT and plant parameters. Due to the volume of sensitivity studies required to support the CSAU step on defining the assessment matrix, minimizing the calculational run time allowed us to be more efficient in this task. Appendix D presents the 3-loop sample problem, this calculation provides the LOCA simulation through whole core quench.

Question 134: *Fig C.1 shows a variation of about 50 K during reflood with time step. Please discuss the effect of smaller time steps on PCT.*

Response 134: In reading Figure C.1, clad temperatures do vary within a band of about 50 K (90°F). As reported in Appendix C, the actual variation of PCT is only []. PCT is the figure of merit in this study. Basically, the current time steps used for RLBLOCA analysis is at the tolerance threshold for reasonable run times. Smaller time steps have been investigated; however, no improvement in numerical uncertainty has been observed.

Question 135: *Please support the basis for the uncertainty, especially the difference between the 95/95 and 50/50 and the data base used to assess the code predictive capability (for example, there are many more FLECHT-SEASET, FLECHT Cosine and FLECHT Skewed tests with PCT between 2000 and 2200 F that were not used in the S-RELAP5 comparisons). This would include the sensitivity of PCT to nitrogen injection, fuel swell and rupture modeling, sensitivity to time step, downcomer boiling sensitivities, etc. If a larger database was used, how would the uncertainty be impacted?*

Response 135: It is fully recognized that there are a significant number of tests that have been performed that were not modeled and analyzed in this methodology submittal. The submittal followed the CSAU approach of identifying the important transient and plant phenomena through the PIRT process. Following the completion of the PIRT an assessment matrix was developed to support evaluation of the important PIRT phenomena, defined as those ranked 5 or higher. This assessment matrix was then evaluated and uncertainties developed and conservatism justified. The most likely result of using a larger database is that the uncertainties would decrease.

Question 136: *As identified on page 3-17 of EMF-2100, the Weber number is used to define the maximum bubble size. For reflood calculations, Wallis has proposed a formula-based on Taylor instability theory. Please discuss the impact of the Wallis approach for choosing bubble size on level swell and reflood behavior and justify the model.*

Response 136: The bubble size is of little importance for the reflood since the bubbly-slug flow occurs only below the quench front. Also, as is pointed out in Response to Question 71a, the adequacy and applicability of the bubbly-slug interphase model for the reflood calculation has been demonstrated in the excellent code-data comparison of the differential pressure below the quench front (Figures 3.3.71 to 3.3.79 of EMF-2102(P) Revision 0). Since the effects are of little importance and the existing model is shown to be adequate, Framatome ANP does not feel that the effort of incorporating a new model such as proposed by Wallis is warranted.

Question 137: *Regarding the critical Weber number of 4.0 for droplets in dispersed flow (page 3-17 of EMF-2100), Wallis recommends that a Weber number of 12 be used to define the maximum drop diameter for viscous fluid droplets. Drop diameters of about 1/10 inch characterize LOCA reflood behavior and have been used to capture the PCT in the FLECHT tests. Please justify the Weber number used to compute the drop size for the FLECHT tests. What is the lower limit on drop size in the S-RELAP5 methodology and how does this value compare to the database?*

Response 137: The critical Weber number and the size of droplets/bubbles are hypothetical processes to obtain reasonable values for interphase friction and interphase heat transfer. The ultimate justification is how good are the code-data comparisons of void distribution, and fluid and surface temperatures. The exact form and interpretation of the critical Weber number relation may vary depending on the application intent and the definition of droplet diameter. In S-RELAP5, the critical Weber number is used to determine a reasonable average droplet diameter. Also, as discussed in Section 3.2.1 of EMF-2100 (P) Revision 4, the critical Weber number is not the only criterion for determining the droplet diameter. An example of droplet diameters calculated by S-RELAP5 during the reflood period is shown in Figure 123.4 (see Response to Question 123). The droplet diameters are mostly in the range between 0.5 mm

and 2.0 mm. Figure 137.1 is a reproduction of a droplet diameter plot for FLECHT-SEASET 31504 from NUREG/CR-2256, "PWR FLECHT SEASET Unblocked Bundle, Forced and Gravity Reflood Task Data Evaluation and Analysis Report," November 1981. It is seen that the S-RELAP5 calculated values, ranging from 0.5 to 2.0mm, are within the data range shown in this figure. Note that the legend "PREDICTION" in the figure is not an S-RELAP5 prediction. The S-RELAP5 calculation is shown in Figure 123.4 (Response to Question 123).

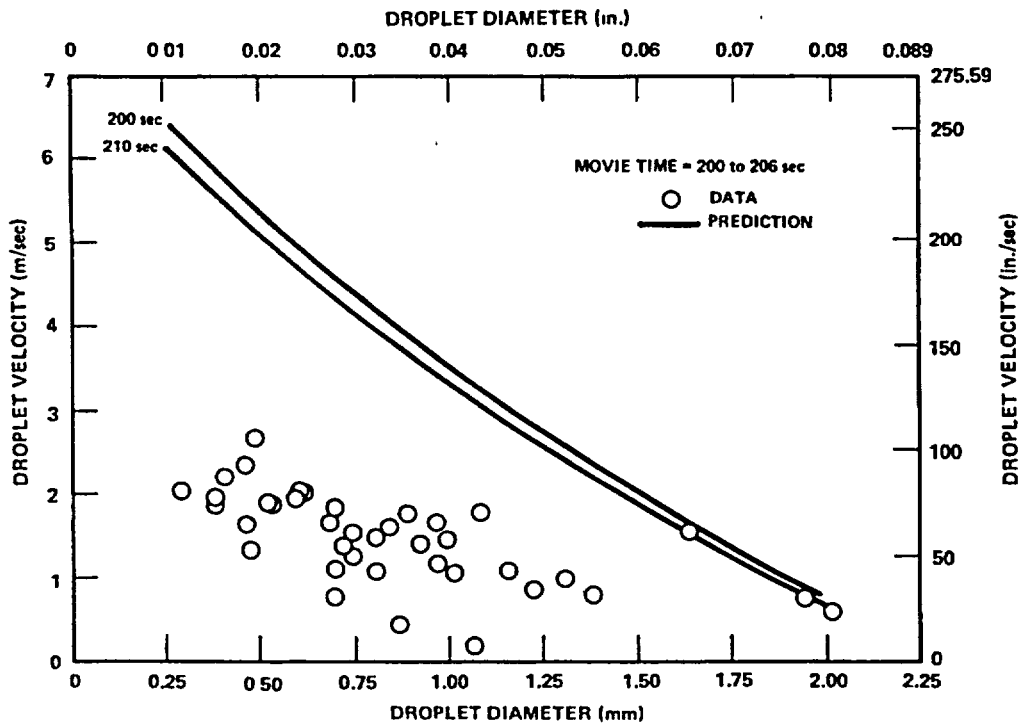


Figure 137.1 Reproduction of Plot of Comparison of Calculated and Measured Drop Velocities, Run 31504, 1.83 m (72 in.) Elevation, Page F20 of NUREG/CR-2256

Question 138: *How are the flow regime maps applied to the 2-D downcomer model?*

Response 138: The flow regime map for 2-D components is discussed in Section 3.1 and in the text below Equation (3.11) of EMF-2100(P) Revision 4. In essence, for the 2-D downcomer, the axial direction parameters are used for determining the flow regime map and the range of the annular-mist regime is expanded.

Question 139: *Since flow regimes affect entrainment and ECC bypass, how was the uncertainty in the flow regime maps included in the methodology?*

Response 139: There is no direct treatment of the uncertainty in the flow regime maps used in the code. Variations between the code predicted flow regime and the actual flow regime is included in the uncertainties generated and conservatisms demonstrated in the other parameters, for example heat transfer coefficients. In the development of the code uncertainties the differences between the code prediction and the experimental data would include differences in the flow regime map. Thus, the uncertainty in the flow regime maps is indirectly included in the statistical treatment.

Additional Items.

Item 1: Two Phase Pump Degradation Model

An evaluation of the use of either the Semiscale or EPRI-CE two phase pump degradation model in the RLBLOCA methodology is presented in Appendix B of EMF-2103(P). The original decision was to use the Semiscale two phase pump degradation model. This decision was based on the fact that the sensitivity study showed an 18 degree F higher PCT using the Semiscale model than the PCT using the EPRI-CE model. Since the expected variability in an S-RELAP5 calculation is approximately 30 degrees F this degree of variation, 18 degrees, indicates that either model will produce the same result in a LBLOCA analyses. Framatome ANP uses the EPRI-CE two phase pump degradation model in its SEMPWR-98 evaluation model and other S-RELAP5 based models. In order to use consistent models in the future, Framatome ANP will use the EPRI-CE two phase pump degradation model in the RLBLOCA methodology.

Item 2: Gadolinia Bearing Fuel Rod Modeling

In the performance of sensitivity studies required to respond to the RAI on the realistic LBLOCA, Framatome ANP discovered that the modeling of gadolinia bearing fuel rods had been performed incorrectly. The modeling of gadolinia fuel rods was corrected and the results showed about a 63F reduction in the 95/95 PCT for the three loop sample problem and a 66F reduction in the four loop sample problem.

[

]

Item 3: NRC Requested Break Size Evaluation

To evaluate the impact of statistically treating the break size in the Framatome ANP proposed Realistic large break LOCA methodology the NRC requested that a sensitivity study on the calculated highest PCT case for the 3-loop plant be performed. The staff specifically requested that the break size associated with the highest reported PCT in EMF-2103 Appendix D, the 3-loop 0.66 DEG cold leg break, be fixed and that the 59 cases be rerun with the other parameters selected by Monte Carlo methods as specified in the methodology.

The 59 cases have been run as requested and the resulting PCTs are provided in Table 1. These cases have all been run with the same break size as EMF-2103 Appendix D case 41, which is the limiting case from the reported 3-loop sample problem with a break size of .66 DEG and a PCT of 1853 F. As shown in the table only two cases from the sensitivity study, case 11 and case 51, have higher PCTs than the limiting case 41 in EMF-2103 Appendix D. The sensitivity study case 51 has a PCT of 1873 F, which is 20 F higher, and case 11 has a PCT of 1929 F, which is 76 F higher.

A comparison was made between EMF-2103 Appendix D case 41 and the sensitivity study case 11 to determine the principle parameters contributing to this difference. The comparison is provided in Table 2 for the most important parameters with respect to their contribution to the PCT. These parameters were selected because they have been shown, based on sensitivity studies, to have the largest impact on PCT. As shown in Table 2, the primary differences which contributed to the higher PCT in the sensitivity study case 11 are the power parameters. Case 11 has a higher Fq and a higher peaked axial shape than the limiting case 41 in EMF-2103 Appendix D.

An additional break spectrum study was also performed by Framatome ANP to look at variations in the break size for EMF-2103 Appendix D case 41, the limiting case from the 3-loop sample problem. The results of this study are provided in Table 3 which looks at a range of guillotine and split breaks. As shown in Table 3, the PCT was reduced for all larger and smaller break sizes relative to the 0.66 guillotine break in EMF-2103 Appendix D case 41. This shows that the EMF-2103 Appendix D case 41 break size is the limiting break size for the statistically selected conditions.

In conclusion, it has been demonstrated for the 3-loop sample problem, that performing a statistical analysis around the break size for the limiting PCT case, EMF-2103 Appendix D case 41, results in only a 76 F change in the maximum PCT. This change is due to a more conservative selection of the Fq and ASI. It has also been demonstrated, that the limiting case for the 3-loop sample problem was associated with the limiting break size given the other selected statistical conditions in EMF-2103 Appendix D case 41.

Table 1 Peak Clad Temperatures for 59 Cases with Constant Break Size – Sensitivity Study

Case Number	Peak Clad Temperature, F
1	1671.4
2	1448.7
3	1675.3
4	1501.4
5	1655.5
6	1651.1
7	1679.1
8	1647.5
9	1733.5
10	1673.9
11	1929.0
12	1802.6
13	1746.8
14	1655.6
15	1720.8
16	1634.1
17	1539.3
18	1588.6
19	1618.1
20	1658.7
21	1515.3

Case Number	Peak Clad Temperature, F
22	1532.1
23	1827.5
24	1477.5
25	1560.1
26	1729.6
27	1504.4
28	1849.9
29	1647.7
30	1358.1
31	1610.5
32	1538.4
33	1685.7
34	1482.5
35	1638.6
36	1675.2
37	1435.6
38	1534.5
39	1584.3
40	1645.1
41	1852.8
42	1804.5
43	1468.5
44	1674.0
45	1628.0
46	1718.0
47	1658.3
48	1720.4
49	1654.9
50	1662.4
51	1872.1
52	1579.2
53	1559.5
54	1517.4
55	1676.4
56	1563.7
57	1619.8
58	1502.0
59	1352.0

Table 2 Comparison of Sensitivity Study Case 11 and EMF-2103 Appendix D Case 41 Parameters

Statistical Parameter	EMF-2103 Appendix D Case 41	Sensitivity Study Case 11
Axial Shape Index (ASI)	-0.0088	-0.1361
Fq	2.28	2.38
Heat Transfer Multiplier, FILMBL	0.8813	1.274
Heat Transfer Multiplier, FRHTC	1.059	1.492

Table 3 Break Spectrum Study for EMF-2103 Appendix D Case 41

Break Type	Break Size	Peak Clad Temperature, F
Guillotine	1.0	1703
Guillotine	0.9	1708
Guillotine	0.8	1742
Guillotine	0.66	1853
Guillotine	0.5	1617
Split	1.0	1607
Split	0.7	1687
Split	0.4	1313
Split	0.1	1226

Appendix A Inverse Heat Conduction Model

Due to the complications resulting from the heater rods being constructed of multiple material layers and the specification of an internal boundary condition via a table of measured values, it is necessary to use a numerical solution to infer the transient surface heat flux. Also, due to the large axial spacing of the rod thermocouples, it is only practical to employ a one-dimensional treatment of conduction within the rod. Thus, all effects of axial conduction will be ignored. This assumption is reasonable under most conditions but it will lead to potential errors in the estimation of the surface heat flux in the vicinity of the quench front. However, because the focus here is to determine heat transfer coefficients in the film boiling region, this assumption is not a major limitation.

There are four principal steps in developing a generalized form for the numerical implementation of the inverse conduction algorithm. First, the transient conduction equation must be put into finite difference form (Section 1.0), then the appropriate internal boundary conditions must be applied (Section 2.0). The resulting matrix solved (Section 3.0) for the transient radial temperature profile. Finally, from the calculated radial temperature profile, the surface heat flux and the heat transfer coefficient are determined. However, as described in EMF-2102, Section 5.1.2.1, it is beneficial (if not necessary) to first pre-condition the thermocouple signal to reduce noise and to also smooth the resulting heat transfer coefficient.

2.0 Finite Difference Equation

The one-dimensional transient radial conduction equation is

$$\rho c_p \frac{\partial T}{\partial t} = \frac{1}{r} \frac{\partial}{\partial r} \left(kr \frac{\partial T}{\partial r} \right) + q''' \quad (1)$$

where

- ρ = Material density, kg/m³
- c_p = Material specific heat, J/kg-K
- k = Material thermal conductivity, W/m-K
- r = Radial location from rod center, m
- $T(r)$ = Material temperature, K
- q''' = Volumetric heat generation rate within the material, W/m³

To formulate a numerical model, a radial noding scheme must be chosen and the conduction equation volume (or area) averaged for each of the nodes. One way of accomplishing this is to divide the conductor into a number of concentric radial rings. For accuracy, the nodal points are placed at the geometric centers of each radial ring. Also, when multiple material regions exist, as

is the case in fuel rod simulators, the radial rings are chosen so that their boundaries coincide with the material boundaries. Within each material region, however, any integral number of radial rings can be specified in order to provide for a finer discretization in regions of sharp temperature gradients.

An important assumption in the implementation of the inverse heat conduction equation calculations is that the presence of the thermocouples within the test rods does not have a major impact on the radial temperature profile in the rods.

An exception to the above is made for the radial ring at the external surface of the fuel rod simulator. This last node is taken to be "half-thickness" so that the actual nodal point is located on the surface. A typical noding scheme for a fuel rod simulator is given in EMF-2102, Figure 5.1. In this example, there are four material regions with a varying number of radial nodes for each region. Note the placement of the last node on the rod external surface.

For the *i*th radial ring, the cross-sectional area averaged transient conduction equation becomes

$$(\rho c_p A)_i \frac{\partial T_i}{\partial t} = K_{i+1/2} (T_{i+1} - T_i) + K_{i-1/2} (T_{i-1} - T_i) + q'_i \quad (2)$$

where

- A_i = Cross-sectional area of the *i*th ring, m²
- K = Inter-node conductance, W/m-K
- q'_i = Linear heat generation rate for the *i*th radial ring, W/m

The inclusion of the subscript "*i*" indicates that the value is either the nodal value (in the case of temperature) or is the area averaged value for that radial ring. The inter-node conductance between node "*i*" and node "*i*+1", denoted as $K_{i+1/2}$, is defined in terms of the thermal resistance as

$$K_{i+1/2} = \frac{1}{R_{i+1/2} + R_{i+1+1/2}} \quad (3)$$

where $R_{i+1/2}$ is the resistance to heat flow from node "*i*" to the boundary between nodes "*i*" and "*i*+1" which is indicated by the subscript "*i*+1/2". Similarly, $R_{i+1+1/2}$ is the thermal resistance between node "*i*+1" and the boundary between nodes "*i*" and "*i*+1". It remains to define the values for these thermal resistances.

To rigorously formulate these resistances, one must know the radial temperature distribution. Since this is the quantity we wish to solve for, a way to approximate these resistances is required. The method used here is to approximate the transient thermal resistance by its steady state value. Thus,

$$R_{i,i+1/2} = \frac{\ln\left(\frac{r_{i+1/2}}{r_i}\right)}{2\pi k_i} \quad (4)$$

where

r_i = The radius of the node center, m

$r_{i+1/2}$ = Radius of the boundary, m

The inter-node conductances are then

$$K_{i,i+1/2} = \frac{2\pi k_i k_{i+1}}{k_{i+1} \ln\left(\frac{r_{i+1/2}}{r_i}\right) + k_i \ln\left(\frac{r_{i+1}}{r_{i+1/2}}\right)} \quad (5)$$

and

$$K_{i-1/2,i} = \frac{2\pi k_i k_{i-1}}{k_i \ln\left(\frac{r_{i-1/2}}{r_{i-1}}\right) + k_{i-1} \ln\left(\frac{r_i}{r_{i-1/2}}\right)} \quad (6)$$

To complete the numerical model, it remains to specify the temporal discretization and to state how the material properties are to be evaluated.

A fully implicit scheme for temporal discretization was implemented. The discretized transient heat conduction equation is

$$\left(\rho^n c_p^n A\right)_i \frac{T_i^{n+1} - T_i^n}{\Delta t} = K_{i,i+1/2}^n (T_{i+1}^{n+1} - T_i^{n+1}) + K_{i-1/2,i}^n (T_{i-1}^{n+1} - T_i^{n+1}) + (q')_i^n \quad (7)$$

where the superscript "n+1" indicates that the quantity is to be evaluated at the new time and "n" at the old time. As indicated above, the material properties are evaluated at the old time value of the nodal temperature.

3.0 Inverse Heat Conduction Equation Boundary Conditions

In a normal transient conduction solution of a fuel rod simulator (cylindrical geometry), there are two boundary conditions: an adiabatic boundary condition for the heater rod centerline and a heat transfer coefficient on the external surface. For the inverse conduction solution, the adiabatic centerline boundary condition is retained. An internal temperature boundary condition is applied at the location of the thermocouple of interest. Implicit to the use of an internal temperature boundary condition is the observation that the thermocouple is present within the test rod. It is assumed that the presence of thermocouples within the test rod does not have a

significant effect on the radial temperature profile. The surface heat flux (or heat transfer coefficient) is one of the unknowns to be determined.

To simplify the discussion, introduce the following notation for the transient conduction equation for the i th node

$$a_i T_{i-1}^{n+1} + b_i T_i^{n+1} + c_i T_{i+1}^{n+1} = d_i \quad (8)$$

where all of the temperatures are at new time and their coefficients are

$$\begin{aligned} a_i &= -K_{i-1/2} \\ c_i &= -K_{i+1/2} \\ b_i &= \frac{(\rho c_p A)_i}{\Delta t} - a_i - c_i \end{aligned}$$

The explicit right-hand-side term is given by

$$d_i = \frac{(\rho c_p A)_i}{\Delta t} T_i^n + q'_i$$

Let the nodes be numbered from 1 to N , where N is the index of the node on the clad exterior surface. The adiabatic centerline boundary condition is applied to the first node by setting

$$a_1 = 0 \quad (9)$$

so that the first conduction equation is reduced to

$$b_1 T_1 + c_1 T_2 = d_1 \quad (10)$$

For the last node, the conduction equation becomes

$$a_N T_{N-1} + b_N T_N = d_N - q''_w P \quad (11)$$

where the wall heat flux, q''_w , and perimeter, P , have been introduced.

If the wall heat flux (or equivalently the heat transfer coefficient) were known, we would now have a set of N equations with N unknown values of the new time temperature forming a tri-diagonal matrix. The solution would then be performed by a straightforward Gaussian elimination and back-substitution. However, because the wall heat flux is one of our unknowns, another boundary condition must be introduced.

Typically, the rod thermocouple would be attached to the inside clad surface. That is, it would be at the boundary between two material regions and hence at the boundary between two

cylindrical rings. Let the ring just inside this boundary be denoted by the subscript "n", so that the boundary is at "n+1/2" and the first node within the clad has the subscript "n+1". Since the location of the measured temperature, T_{meas} , to be used as a boundary condition does not coincide with the location of one of our nodes, it cannot be used directly as a temperature boundary condition. Instead, because a boundary cannot store energy, a constant heat flux boundary condition across this interface is applied. That is,

$$q''_{n,n+1/2} = q''_{n+1/2,n+1} \quad (12)$$

where

$$q''_{n,n+1/2} = \text{heat flux from node "n" to the boundary}$$

$$q''_{n+1/2,n+1} = \text{heat flux from the boundary to node "n+1".}$$

In terms of the thermal resistances introduced above,

$$\frac{T_n - T_{meas}}{R_{n,n+1/2}} = \frac{T_{meas} - T_{n+1}}{R_{n+1/2,n+1}} \quad (13)$$

where all of the temperatures are at the new time. Equation (13) can be recast as

$$b'_n T_n + c'_n T_{n+1} = d'_n \quad (14)$$

where

$$b'_n = \frac{1}{R_{n,n+1/2}}$$

$$c'_n = \frac{1}{R_{n+1/2,n+1}}$$

$$d'_n = (b'_n + c'_n) T_{meas}$$

Equation (14) is the implementation of the internal boundary necessary to provide for the determination of the surface heat flux. Section 4.0 describes the solution procedure for the new time nodal temperatures.

4.0 Inverse Heat Conduction Equation Solution Procedure

There are N+1 equations (N transient conduction equations plus the interface heat flux constraint) and N+1 unknowns (N new time temperatures and the surface heat flux). Therefore, the system is solvable. To do so, the solution is divided into two parts.

the heat transfer coefficient rather than the measured thermocouple temperature. Thus, the resulting heat transfer coefficient is consistent with that computed in S-RELAP5.

Appendix B Quench Time Determination in Measured Data

The criteria applied to determine quench time in the THTF and FLECHT-SEASET tests are different. The differences are caused by the difference in data sampling rates and also because the FLECHT-SEASET algorithm was optimized for low pressure reflood conditions.

FLECHT-SEASET Quench Determination

The FLECHT-SEASET criteria are taken from Reference 1 (from page E-26 of the report). The algorithm examines five sequential data points at a time. These temperature points are identified by index, i.e., $T(i)$, $T(i+1)$, $T(i+2)$, $T(i+3)$, and $T(i+4)$. They are associated with time $t(i)$, $t(i+1)$, $t(i+2)$, $t(i+3)$, and $t(i+4)$, as shown in Figure B.1.

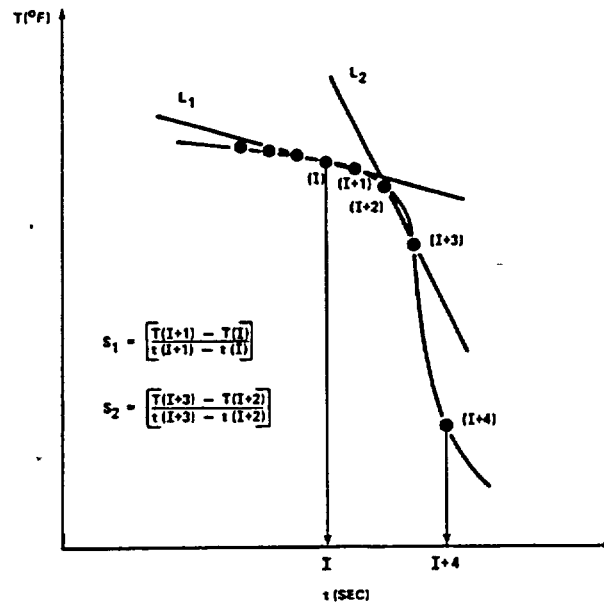


Figure B.1 FLECHT-SEASET Quench Analysis (Figure E-1 from Ref. 1)

The algorithm is performed in steps. In the first step, the temperature $T(i)$ must be greater than 149°C for a potential quench condition to exist.

In the second step, quench may exist if the slope of the temperature time curve between the third and fourth points is greater than 28°C/S .

$$S_{L2} = \frac{T(i+3) - T(i+2)}{t(i+3) - t(i+2)} < -28 \text{ } ^\circ\text{C/s}$$

In the third step, if the absolute value of the slope between the third and fourth points is more than two times greater than the absolute value of the slope between the first two points, then a potential quench condition exists.

$$S_{L1} = \frac{T(i+1) - T(i)}{t(i+1) - t(i)}$$

$$|S_{L2}| > 2|S_{L1}|$$

In the fourth step, provided all of the above criteria have been satisfied, and if the slope between the fourth and fifth points is greater than the slope between the third and fourth points, then quench is determined to have occurred.

$$S_{L3} = \frac{T(i+4) - T(i+3)}{t(i+4) - t(i+3)}$$

$$|S_{L3}| > |S_{L2}|$$

In the fifth step, the time and temperature of quench is calculated to be the intersection between the lines L_1 and L_2 .

THTF Quench Determination

The FLECHT-SEASET algorithm was specifically developed for low pressure reflood conditions and for thermocouple traces with low sampling frequencies. Indeed, several of the criteria used to find the quench condition are, in effect, hardwired for the conditions expected in FLECHT. Consequently, they do not work at all for the high pressure conditions of the THTF reflood tests.

One possible approach would be to find another set of hardwired criteria to be implemented in a THTF version of the algorithm. But the relatively high sampling frequencies of the THTF data, 20-100 Hz, allows another, more mathematical, approach.

For pool boiling, T_{min} is defined to occur at a local minimum in the surface heat flux for which the heat flux begins to increase as the wall temperature is reduced. For this special case (constant fluid conditions), the criteria for T_{min} can be expressed as:

$$\frac{dq''}{dT_w} = 0 \text{ with } T_w > T_{CHF}$$

In theory, one could perform just such a test for the THTF data. However, in quenching tests, the fluid conditions change dramatically with time, i.e., from superheated vapor to subcooled liquid, and so the derivative of the surface heat flux can be confounded due to the change in fluid conditions. Therefore, another set of criteria is needed.

In a quenching test, the quench temperature is associated with the "knee" in the thermocouple trace (Figure B.2).

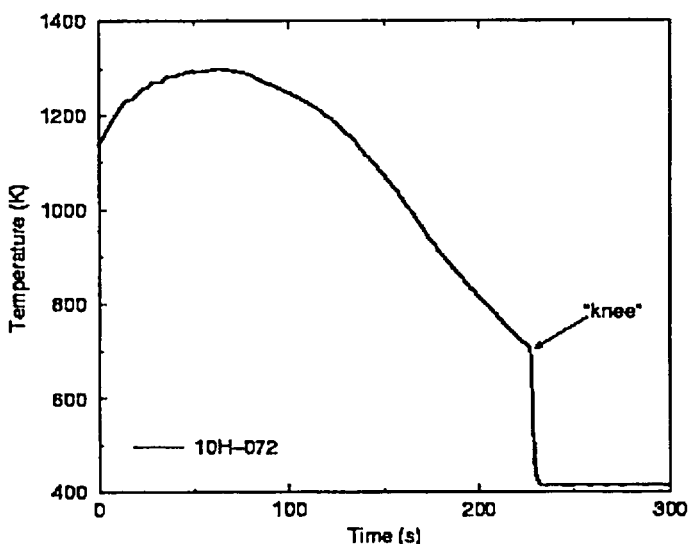


Figure B.2 Illustration of the "Knee" in a Thermocouple Trace

The physical reason for this "knee" is that as the wall temperature decreases, it reaches a point where heat transfer to the liquid can begin and subsequent decreases in the wall temperature accelerate the process. The result is a pronounced change in the slope of the thermocouple trace thereby creating the "knee" in the curve. The quench condition can then be identified by searching for the location of the maximum change in slope of the thermocouple trace, or in other words, by finding the location of the most negative value of the curvature:

$$\min \left[\frac{\partial^2 T_w}{\partial t^2} \right] \Rightarrow t_q \text{ and } T_q$$

The second derivative of temperature with respect to time for the *i*th data point is then approximated by the finite difference form:

$$\frac{\partial^2 T_w}{\partial t^2} \approx \frac{T_{i+1} - 2 \cdot T_i + T_{i-1}}{2 \cdot \Delta t}$$

where, T_i is value of thermocouple temperature for the *i*th data point and Δt is the time step size between data points.

Using this criteria, the time, t_{max} for which the maximum negative value of the curvature has been found indicates that the rod has already begun quenching by this time in the transient. So, if the quench time and quench temperature are assigned as the recorded values at this point, that is, $t_Q = t_{max}$ and $T_Q = T_{max}$, then the calculated quench time should be slightly later than the actual quench time and the quench temperature slightly below its actual value. The time differential is minimal as the time step size in THTF is either 0.01 or 0.05 seconds. However,

despite the miniscule difference in quench time, due to the extremely high rate at which the clad temperature is decreasing (> 400 K per second), the under-estimation of the quench temperature can be on the order of 25 K.

In calculating the quench temperature there are two other complications that should be considered:

- The thermocouple signal is noisy and to prevent false indications of quenching, the signal has been filtered before it was analyzed. How much does this filtering distort the value of the quench temperature?
- The quench temperature is based on the filtered thermocouple signal and the thermocouple is located on the interior of the clad surface. How much does the actual clad surface temperature differ from the thermocouple reading?

The following two figures illustrate the temperature differences that can result from filtering the thermocouple signal. In the first, Figure B.3, there is no discernable difference between the original and the filtered signal. At an extremely fine scale focused on the quench point (Figure B.4), it is observed that the filtered signal has a smoother shape and under-predicts the temperature at the point of maximum negative curvature. For this particular example, the temperature difference is ~ 9 K. Of course, the exact value of this under-prediction varies from thermocouple to thermocouple and from test to test, however, this example gives a good indication of the trend towards under-prediction and its approximate magnitude.

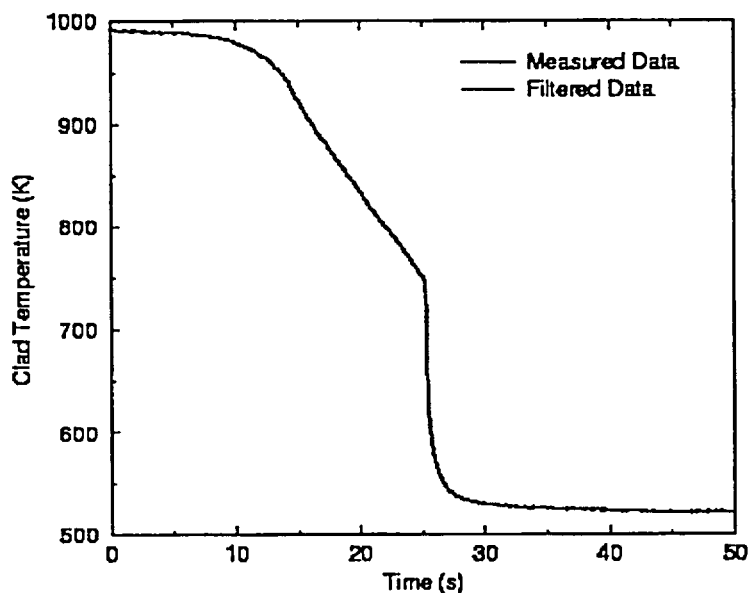


Figure B.3 Comparison of Original Thermocouple Signal and the Filtered Signal for Thermocouple TE-320AG of Test 3.02.10C

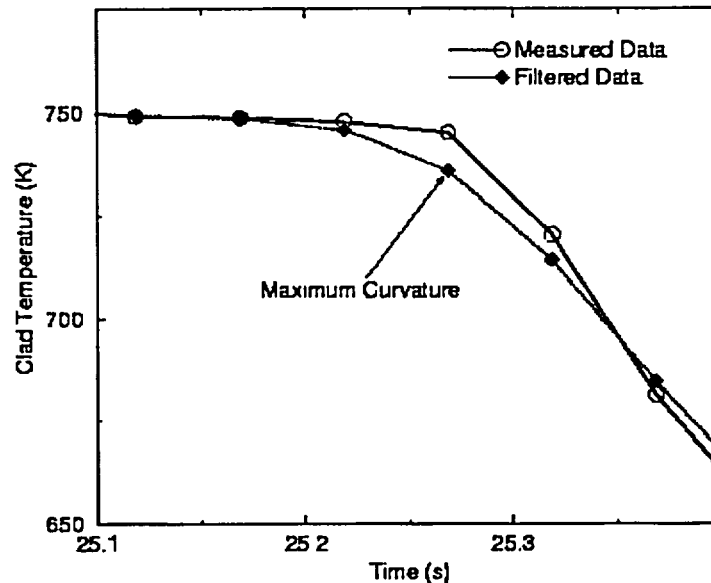


Figure B.4 Detail of the Comparison of Original Thermocouple Signal and the Filtered Signal for Thermocouple TE-320AG of Test 3.02.10C Showing Location of the Point of Maximum Negative Curvature

In the S-RELAP5 heat transfer package, the wall temperature criterion for the transition from the film boiling regime to transition boiling is based on the temperature of a node located on the rod surface. In contrast, reported quench temperatures are normally based on a thermocouple reading where the thermocouple is attached to the clad interior. This was the case for the quench temperatures computed by the data analysis program for the FLECHT-SEASET tests and is also the case for the high pressure THTF reflood tests. Consequently, there is the potential to introduce a non-conservative bias as the measured temperature will always be greater than the actual clad surface temperature.

Usually, it is argued that up until the time of quench the rod heat flux is low (on the order of the decay heat) and this, combined with the high thermal conductivity of the clad material, results in a small temperature drop across the clad that is negligible compared to the uncertainty in determining the quench temperature. That this is indeed the case is illustrated in Figure B.5. The plotted thermocouple signal is the same filtered signal that is used in both the quench temperature analysis and as the boundary condition in the inverse conduction solution for the heat transfer coefficient. The plotted surface temperature is that which results from the inverse conduction solution.

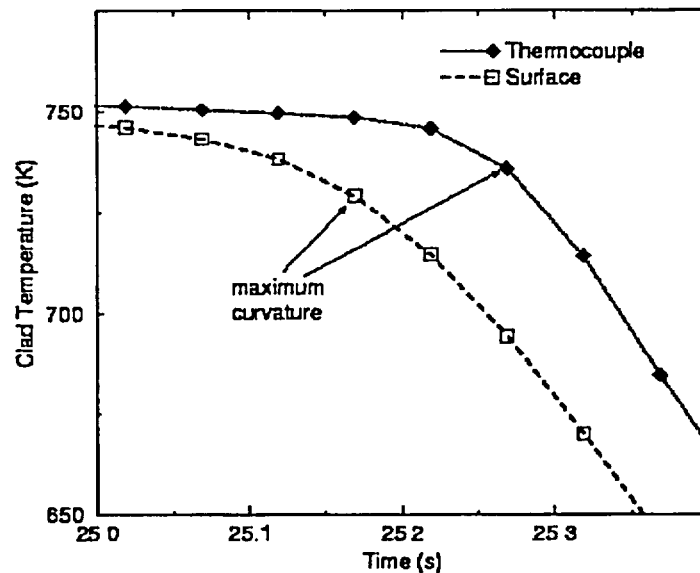


Figure B.5 Comparison of Calculated Surface Temperature with Thermocouple Response for Thermocouple TE-320AG of Test 3.02.10C at the Onset of Quenching

Before the arrival of the quench front, the temperature drop across the clad is on the order of 5 K. During quenching, the thermocouple response lags behind the surface response by about 0.1 seconds. So, at any given point in time, the clad temperature drop can approach 50 K. However, if one compares the points of maximum negative curvature on the two curves, there is a time shift of 0.1 seconds but the calculated quench temperature differs by less than 10 K. To some extent, this over-prediction counter balances the bias towards under-prediction introduced by the signal filtering and by selecting the point with maximum curvature as the quench point. Although it would be a difficult exercise to quantify the magnitude of each of these three effects, based on the above, it appears reasonable to take the quench temperatures calculated by the data analysis program as a lower bound to the actual quench temperatures and to use the spread in the data as an estimate of their uncertainty.

Reference

1. "PWR FLECHT-SEASET Unblocked Bundle, Forced and Gravity Reflood Task Data Report, Volume 1," NUREG/CR-1532, June 1980.

Appendix C
Changed Pages for Section 5 of EMF-2103

]

[

]

5.2.2 Application of Methodology

The FRA-ANP RLBLOCA methodology is a statistics-based methodology; therefore, the application does not involve the evaluation of different deterministic calculations. [

] The methodology results in a bounding value with 95% probability and 95% confidence in the PCT.

The PCT criterion is shown to be met with at least 95% probability and 95% confidence by comparing the 95/95 PCT value to the PCT criterion. Regulatory Guide 1.157 states that it is not necessary to explicitly consider the probability of meeting the other 10 CFR 50.46 criteria due to the strong dependence of the other criteria on PCT. Demonstration that the PCT criterion is met with 95% probability and 95% confidence shows that the other criteria are also met with high probability as required by the regulation. In order to define values for peak local oxidation and total core oxidation, these values will be reported from the 95/95 PCT case.

Application of this methodology relies on two computer codes: RODEX3A and S-RELAP5. All key LBLOCA parameters are calculated from S-RELAP5; RODEX3A is used to generate the initial fuel properties to be used by the fuel performance models in S-RELAP5. Performance of the RLBLOCA calculations relies on three analyst-created code input files describing the fuel, plant thermal-hydraulics, and containment thermal-hydraulics. The fuel model input is

The parameters treated statistically are listed in Table 5.6 and the values for the specific parameters and ranges addressed are given in Table 5.7. The distributions assumed for this sample problem are those given in Table 5.4. [

] The results of these calculations are presented in Figures 5.2 through 5.28.

Figures 5.2 through 5.16 present scatter plots for the more important phenomena/parameters in the analysis. These scatter plots are provided to demonstrate that the methodology does select input which covers the phenomena/parameter ranges and associated distributions. In general, it is difficult to see the PCT dependence of an individual parameter from these scatter plots. This is primarily due to the fact that there are several major parameters and a conservative combination of these parameters is required to obtain the higher values of PCT. Based on this the following paragraphs will concentrate on a discussion of the LBLOCA criteria as addressed by the analysis.

[

]

[

]

[

]

[

]

[

]

[

]

[

]

[

]

[

]

[

]

5.4 *Determination of Total Uncertainty (CSAU Step 14)*

[] the biases and uncertainties determined during the code assessments are either directly addressed in the statistical analysis or demonstrated to be a code conservatism which adds an additional unquantified conservatism to the reported results. The final results for the 4-loop sample problem can be summarized as follows:

- The 95/95 calculated PCT was 1686 F which compares to the criterion for maximum PCT of 2200°F.
- The maximum nodal oxidation for the 95/95 PCT case was 0.8% which compares to the criterion for maximum nodal oxidation of 17%.
- The maximum total oxidation for the 95/95 PCT case was 0.02% which compares to the criterion for maximum total core oxidation of 1%.

Based on these results, it is concluded that the LBLOCA analysis for the sample W 4-loop plant meets the criteria for the LBLOCA event.

With respect to the identification of the degree of conservatism in the analysis, a comparison can be made to the 50/50 probability value for the PCT. The 50/50 PCT at 1375°F is 311°F less than the 95/95 PCT.

Appendix D
Changed Pages for Two-Phase Pump Degradation Model

with higher flows (54 and 68) the predicted levels are either conservative or in reasonable agreement.

For the UPTF tests, the liquid is separated in the steam generator simulator. For the two tests, the calculated liquid accumulating in the catch tanks is quite conservative (See Figures 4.168 through 4.171).

For the FLECHT-SEASET tests, there is no steam generator. The hot-leg piping terminates in a separator, which has a tank with a pipe in the bottom leading to a drain tank. Figures 4.172 through 4.179 compare the calculated levels in the separator tank and the separator drain tank with the measured levels. Because of the tendency of the model to hold a larger quantity of liquid in the upper plenum initially than would be indicated by measurements (See Section 4.3.3.1.4), the calculated carry-over to the separator is delayed. The bottom line for these figures is that the calculation has the liquid carried over to these tanks arriving slightly later than the measurements would indicate, with the overall carry-over from the calculation being greater. This latter point shows that the liquid entrained and carried over by the hot-leg model is conservative.

4.3.3.1.7 Two Phase Pump Degradation

The pump two phase degradation is addressed in the methodology as a best estimate input. Based on the sensitivity study described in Appendix B for a limiting break on both a 3-loop and a 4-loop plant, it is shown that this is not an important phenomenon for the limiting LBLOCA case. The use of the Semiscale two-phase degradation instead of the CE/EPRI two-phase degradation model produced essentially no impact on the 3-loop results and only an 18 F (10 K) for the 4-loop plant. Thus, the best estimate CE/EPRI model will be used in the RLBLOCA methodology.

4.3.3.1.8 Pump Differential Pressure Loss

The pump differential pressure loss is addressed in the methodology strictly as a best estimate. The S-RELAP5 code has the ability to input the pump specific homologous curves for the NPP being analyzed and this option is used. The homologous curves for the specific NPP pumps are obtained from the utility and, if plant data is available, a pump coast down is modeled to ensure that the curves are consistent with the plant data.

region was tested at full scale in the UPTF, as were the hot legs and the steam generator inlet plenum. The steam generator tubing geometry is prototypic in the CCTF (although the number of tubes is smaller). All these tests in the three facilities collected water carried over from the core under conditions representing the reflood phase of the LBLOCA and all three have additional collapsed liquid level measurements. As presented in Section 4.3, a study on carryover to the steam generator was performed using the CCTF. From that study, a bias on interfacial drag was determined to conservatively bound this phenomenon. The results of the CCTF (with bias), UPTF, and FLECHT-SEASET evaluations indicate that S-RELAP5 overpredicts the entrainment of liquid from the test bundle (Section 5.6 and Reference 5). While each test by itself has some deficiencies in terms of simulating a PWR and in terms of scale, the combination of the three tests provides a substantial basis for evaluating modeling of the drag between the two phases during reflood at full scale.

4.4.2.2.5 Pump Scaling

The S-RELAP5 code has normalized single phase homologous curves for a full scale W reactor coolant pump as code default. The use of full scale data for the pump makes code scaling moot for the pump. These homologous curves are set to applicable values by entering plant specific values for rated head, torque, moment of inertia, etc. The coastdown of the pump is driven by the torque and moment of inertia of the rotating mass. The torque includes the effects of friction and back EMF (pump torque) and of the loop pressure losses (hydraulic torque). The single phase pump head and torque curves are adjusted for two-phase degradation based on experimental data. The EPRI two-phase degradation data (Reference 54) is based on pumps that are similar to PWR coolant pumps and represent best estimate parameters.

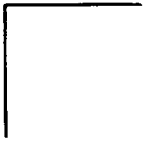
4.4.2.2.6 Cold Leg Condensation

Cold leg condensation was evaluated at a scaled EPRI test facility (Reference 55) to determine the accuracy of the calculated interfacial heat transfer between the ECC water and the steam in the cold leg. The principal portion of the test apparatus was the simulated cold leg, which was fabricated from straight pipe with an ID of 10.42 in. Two injection points were provided so that the pipe lengths downstream of the injection point approximated either a typical PWR cold leg scaled down to about one-third or the full length of the cold leg. The cold leg pipe length

Table 4.1 Parameters Perturbed for PIRT Sensitivity Studies (*Continued*)



Table 4.18 Important PIRT Phenomena and Methodology Treatment



0

|



In the sensitivity studies the single-phase homologous curves ($H_{1\phi}$) used for all cases are supplied by the default Westinghouse pump data that is coded in S-RELAP5. The model describing two-phase degradation (H_{DEGRAD} and $M(\alpha)$) is entered as tabular input to S-RELAP5. For the base case, the default EPRI-CE data (Reference 59) for two-phase degradation is specified. The sensitivity study examined replacing the EPRI-CE degradation model with the Semiscale degradation model. The degradation model is only applied when two-phase conditions are present in the pump. During the rapid blowdown resulting from a LBLOCA, this period lasts about 10-15s following the break.

The PCT results, relative to the three base cases without accumulator nitrogen, are shown in Figures B.13 - B.15 (extracted for the time period of interest). For the 3-loop plant cases, no sensitivity is evident. This is the expected result, since the break size chosen was selected to minimize the enhanced blowdown heat transfer provided by the pumps. The 4-loop plant case does show an increase in the blowdown peak PCT of about 18 °F (10 K).

The PCT change of 18 °F well within the expected variability of the results which is about 30 °F (see Appendix C). In hindsight the pump degradation does not appear to be as significant of a parameter as originally anticipated. This result is consistent with the original work performed on the CSAU methodology (Reference 4). Since it has been demonstrated that increased pump degradation is not an important PIRT phenomena, the best-estimate EPRI-CE degradation model will be used in the RLBLOCA methodology.